

CONTENTS — M

Forsterite-bearing Type B CAIs: Case Studies in Melt Distillation and Hybridization <i>G. J. MacPherson, A. N. Krot, and A. A. Ulyanov</i>	5331
A Magnesian Granulite Clast in Lunar Meteorite ALHA81005 <i>A. K. Maloy, A. H. Treiman, and C. K. Shearer Jr.</i>	5278
Presolar Grains in the Tagish Lake Meteorite <i>K. K. Marhas and P. Hoppe</i>	5184
Concerning the Importance of Recoil in Understanding Presolar Nanograins <i>E. Marosits, J. Maul, and U. Ott</i>	5031
Trapping of Xenon Upon Evaporation-Condensation of Organic Matter Under UV Irradiation: Isotopic Fractionation and Electron Paramagnetic Resonance Analysis <i>Y. Marrocchi, F. Robert, L. Binet, and B. Marty</i>	5212
A New Method for Measuring the Extent of Thermal Metamorphism in Ordinary Chondrites <i>C. A. Marsh, D. S. Lauretta, and K. J. Domanik</i>	5336
Extinct ²⁴⁴ Pu on the Moon <i>K. Marti, C. Black, and K. J. Mathew</i>	5125
Amino Acids Composition and Oxygen Isotopes in the Shisr 033 CR Chondrite <i>Z. Martins, R. C. Greenwood, I. A. Franchi, O. Botta, P. Ehrenfreund, and B. A. Hofmann</i>	5164
Noble Gases in the Newly Found Diderot Chassignite <i>B. Marty, A. Grimberg, V. S. Heber, and R. Wieler</i>	5175
Spectra and Petrography of Eucrites as a Guide to Asteroidal Basalts <i>R. G. Mayne, J. M. Sunshine, T. J. McCoy, and H. Y. McSween Jr.</i>	5174
Melt REE Contents of Lherzolithic Shergottite ALH77005 and Nakhlite MIL03346: Application of the Eu-Oxybarometer <i>M. C. McCanta, M. J. Rutherford, and C. Calvin</i>	5249
The Early Crystallization History of the Aubrite Parent Body <i>T. J. McCoy, A. Gale, and T. L. Dickinson</i>	5146
Minor Element Zoning in Nakhrites: What's Going On? <i>G. McKay and T. Mikouchi</i>	5335
Odyssey GRS and SNC Meteorite Evidence for Multiple LIL-enriched Reservoirs on Mars <i>S. M. McLennan, B. C. Hahn, W. V. Boynton, and G. J. Taylor</i>	5251
Fission Xenon in Trinitites <i>A. P. Meshik, O. V. Pravdivtseva, and C. M. Hohenberg</i>	5321
Pre- and Post-Supernova Nucleosynthesis of Cosmochemically Significant Isotopes in Massive Stars <i>B. S. Meyer</i>	5094

Comparative Mineralogy of Chassigny and NWA2737: Implications for the Formation of Chassignite Igneous Body(s) <i>T. Mikouchi</i>	5240
SEM-EBSD Analysis on Symplectic Inclusion in the QUE93148 Olivine <i>T. Mikouchi and K. Righter</i>	5113
Inside of the Flynn Creek Impact and Processes of Central Uplift Formation: The View from Hawkins Impact Cave <i>K. A. Milam, B. Deane, P. L. King, P. C. Lee, and M. Hawkins</i>	5221
Rb-Sr and Sm-Nd Isotopic Systematics of NWA 2737 Chassignite <i>K. Misawa, C.-Y. Shih, Y. Reese, L. E. Nyquist, and J-A. Barrat</i>	5200
Origin of Main-Group Pallasites <i>D. W. Mittlefehldt</i>	5025
A New Iron-Nickel Phosphide from the Northwest Africa 1054 Meteorite <i>V. Moggi Cecchi, L. Bindi, and G. Pratesi</i>	5308
Mid-Infrared Spectroscopy of Matrix Materials from Chondrites: First Heating Experiments <i>A. Morlok, M. Koehler, and M. M. Grady</i>	5237
Revised Dating of Alamo and Some Other Late Devonian Impacts in Relation to Resulting Mass Extinction <i>J. R. Morrow and C. A. Sandberg</i>	5148
Eu Isotopic Variations in Allende CAI <i>F. Moynier, A. Bouvier, J. Blichert-Toft, P. Telouk, D. Gasperini, and F. Albarède</i>	5193
Zn Isotopic Mass Fractionation During High Temperature Segregation of Metal from Silicate <i>F. Moynier, T. Rushmer, and F. Albarède</i>	5223
Extreme Fractionation of Zinc Isotopes in Enstatite Chondrites and Aubrites <i>E. Mullane, S. S. Russell, and M. Gounelle</i>	5134
Fractionation of Iron Isotopes During Magmatic Processing on the IIIAB Parent Body <i>E. Mullane, S. S. Russell, and M. Gounelle</i>	5133
Iron Isotope Compositions of Enstatite Chondrites and Aubrites <i>E. Mullane, S. S. Russell, and M. Gounelle</i>	5135
Experimental Petrology of Olivine-Phyric Shergottites: Primary Mantle Melts? <i>D. S. Musselwhite and A. H. Treiman</i>	5280

FORSTERITE-BEARING TYPE B CAIS: CASE STUDIES IN MELT DISTILLATION AND HYBRIDIZATION. G. J. MacPherson¹, A. N. Krot², and A. A. Ulyanov³

¹Dept. of Mineral Sciences, US National Museum of Natural History, Smithsonian Institution, Washington DC 20560 USA. E-mail: glenn@volcano.si.edu. ²HIGP/SOEST, University of Hawaii at Manoa, Honolulu, HI 96822, USA. ³Moscow State University, Moscow 119992, Russia

Introduction: Two processes that significantly modified materials in the solar nebula were hybridization (combining of different objects into a single composite) and melt volatilization. The importance of both processes is becoming clear, but their nature remains imperfectly understood. E.g., Type B CAIs have compositional, mineralogic, and isotopic features that only recently have been recognized as the result of fractional distillation during the melt phase [1-4]. Studies of rare compound CAI-ferromagnesian chondrule objects are only now shedding light on the origin of some Al-rich chondrules [5-6]. A rare variety of CAIs known as forsterite-bearing Type Bs (FoBs) exhibit far more striking effects of melt volatilization than do Type Bs, and in addition some of their unusual chemical and structural features may reflect hybridization between Type B CAIs and olivine-rich materials. We have begun a comprehensive petrologic and isotopic study of FoBs in order to understand both the origin of their unusual bulk chemistry and mineralogy, and the melt distillation process and the conditions under which it occurred.

Descriptions: The general properties of FoBs – commonly spheroidal shapes, porphyritic textures, mineral chemistry and zoning – suggest that FoBs solidified from melt droplets [7]. However, their appearances are immediately-striking extreme heterogeneity in two different ways. First, their outer mantles are greatly enriched in aluminum and depleted in magnesium relative to their cores, so much so that olivine is commonly missing altogether from the mantles. In fact, the mantles of some of these objects contain an assemblage of gehlenitic melilite, anorthite, and even hibonite that cannot have crystallized from the same melt bulk composition as did the CAI cores [8,9]. The melilite compositions in the core and mantle, for example, represent opposite sides of the thermal minimum in the gehlenite-åkermanite liquidus curve [8]. The second kind of heterogeneity exhibited by FoBs is that, even in the cores, there exist olivine-rich and olivine-poor regions. The inclusions thus have a patchy appearance. Only some of this patchy olivine heterogeneity can be attributed to olivine reacting with the melt to form Åk-rich melilite [e.g. 9].

Discussion: Many FoBs are known to exhibit large mass-dependent isotopic fractionation effects [8], and one is known to be a FUN CAI [9]. The combination of this isotopic evidence, taken together with the presence of an Al-rich mantle whose bulk chemistry is so different from that of the core that the respective mineral assemblages of the two sites are fundamentally incompatible, points strongly toward fractional (Mg, Si) melt volatilization [8,9] that happened on a time scale sufficiently rapid to prevent homogenization of the inner and outer portions of the melt droplets. The bulk compositions of FoBs are approaching to those of Al-rich chondrules, but contain a melilite-rich component that the chondrules lack. This, plus, the patchy olivine distribution, suggests that FoBs are rare cases of hybrids between Type B CAIs and olivine-rich material.

References: [1] Grossman et al. 2000, *GCA* 64: 2879. [2] Grossman et al. 2002, *GCA* 66: 145. [3] Richter F. M. 2004, *GCA* 68: 4971. [4] Richter et al. 2002, *GCA* 66: 521. [5] Scott E. R. D. and Krot A. N. 2001, *MAPS* 36: 1291. [6] Krot et al. 2002, *MAPS* 37: 155. [7] Wark D. A. 1987, *GCA* 51: 607. [8] Clayton R.N. et al. 1984, *GCA* 48: 535. [9] Davis A. M. et al. 1991, *GCA* 55: 621.

A MAGNESIAN GRANULITE CLAST IN LUNAR METEORITE ALHA81005.

A.K. Maloy^{1,2}, A.H. Treiman², and C.K. Shearer Jr.³ ¹Department of Earth Science, Rice University, Houston, TX 77005 (maloyak@rice.edu) ²Lunar & Planetary Institute, Houston, TX 77058 (treiman@lpi.usra.edu) ³Institute of Meteoritics, University of New Mexico, Albuquerque, NM 87131 (cshearer@unm.edu)

Introduction: Granulites are impact-metamorphosed rocks [1] found throughout the lunar highlands [2]. The composition of many lunar granulites cannot be linked to known highland lithologies [3]. Specifically, magnesian granulites ($Mg^* > 70$) are distinct from pristine highland rocks in major and trace element chemistry [4-6]. An additional distinction exists between the magnesian granulites in some feldspathic lunar meteorites and those collected by the Apollo missions [Treiman A.H., unpublished data]. We combine EMP element X-ray maps with EMP and SIMS mineral compositions to reconstruct the bulk chemical composition of a magnesian granulite in ALHA81005.

Sample and Methods: Analyses were performed on a magnesian granulite, Clast 3, in lunar meteorite ALHA81005.48. A compositionally representative field of Clast 3 was selected. Major and minor element X-ray maps, and compositions of major mineral phases in the clast, were acquired with a Cameca SX 100 EMP. The trace element compositions of major mineral phases were obtained by SIMS (Cameca ims 4f) at UNM. Element maps were imported into image-processing software and classified into mineral maps. The proportions of minerals were estimated from the histogram outputs of classifications. Mineral modes were translated into the mass % of each phase, and then combined with mineral compositions to calculate the bulk chemistry of Clast 3 (Table 1).

Results and Discussion: Clast 3 is similar to other magnesian granulites in ALHA81005 [7]. It consists of approximately 66% plagioclase ($An_{97.1}$), 17% low-Ca pyroxene, 14% olivine ($Fo_{81.5}$), 2% augite, and traces of chromite, troilite, and whitlockite. The Mg^* of Clast 3 is 82. From their concentrations in plagioclase, we infer La $\sim 0.8xCI$ and Eu $\sim 9.5xCI$ for bulk Clast 3. Clast 3 is similar to Mg-Suite rocks in plagioclase composition and Mg^* , but is more feldspathic. Estimating Sm from La [6], Clast 3 has Ti/Sm $\sim 4xCI$, which is not in the range displayed by Apollo magnesian granulites. The composition of Clast 3 indicates that magnesian granulites in ALHA81005 are not like Apollo magnesian granulites, and are not simple mixtures of highland rocks in the Apollo sample set.

References: [1] Warner J.L. et al. 1977. *Proceeding of the 8th Lunar Science Conference* 2051-2066. [2] Wood J.A. et al. 1970. *Proceeding of the Apollo 11 Lunar Science Conference* 965-988. [3] Simonds C.H. et al. 1974. *Proceeding of the 5th Lunar Science Conference* 337-353. [4] Lindstrom M.M. and Lindstrom D.J. 1986. *Journal of Geophysical Research* 91(Suppl.): D263-D276. [5] Korotev R.L. and Jolliff B.L. 2001. Abstract #1455. *32nd Lunar & Planetary Science Conference*. [6] Korotev R.L. et al. 2003. *Geochimica et Cosmochimica Acta* 67: 4895-4923. [7] Goodrich C.A. et al. 1984. *Journal of Geophysical Research* 89 (Suppl.): C87-C94.

Table 1

SiO ₂	44.77
TiO ₂	0.15
Al ₂ O ₃	24.08
Cr ₂ O ₃	0.18
FeO	4.59
MnO	0.08
MgO	11.77
CaO	13.95
Na ₂ O	0.22
K ₂ O	0.01
P ₂ O ₅	0.001
S	0.016
Total	99.82
La (x CI)	0.81
Eu (x CI)	9.52

PRESOLAR GRAINS IN THE TAGISH LAKE METEORITE.

K. K. Marhas and P. Hoppe. Max-Planck-Institut für Chemie, 55020 Mainz, Germany. Email: kkmarhas@mpch-mainz.mpg.de.

Introduction: Different types of presolar grains have been identified in primitive meteorites [1]. Tagish Lake is a unique primitive carbonaceous chondrite and the first representative of the CI2 group. It has a fine-grained matrix with olivine-rich aggregates, sparse chondrules, altered CAIs, magnetite, and Ca-Mg-Fe-Mn carbonates (indicating aqueous alteration) [2]. Stepped combustion experiments [2, 3] indicate the presence of presolar grains (SiC, diamonds). From these measurements the matrix-normalized abundance of presolar SiC was estimated to be 8 ppm [3]. In order to explore the inventory of presolar grains in Tagish Lake in more detail we will present here new data from an in-situ search of presolar grains (oxides, silicates, carbonaceous grains) in a polished thin section of Tagish Lake with the NanoSIMS.

Experimental: The NanoSIMS was used in multicollection mode to map two different regions of the fine-grained matrix for two sets of measurements: (i) A search for presolar oxides/silicates ($^{16,17,18}\text{O}$, ^{28}Si , $^{27}\text{Al}^{16}\text{O}$) and (ii) a search for presolar carbonaceous grains ($^{12,13}\text{C}$, $^{26,27}\text{CN}$, ^{28}Si). A < 1 pA Cs^+ primary ion beam, ~ 100 nm in size, was used to raster (256 x 256 pixels) areas of 15 x 15 μm^2 . Each measurement lasted for about one hour and consisted of 4 image layers. A total area of 29,250 μm^2 was mapped for the search of presolar oxide and silicate grains, and 5,400 μm^2 for the search of presolar carbonaceous grains.

Results and Discussion: One presolar silicate grain of ~ 350 nm was found, representing an abundance of ~ 4 ppm of matrix material in Tagish Lake. Although statistics is limited, this is compatible with the abundances inferred for ordinary chondrites [4] but much lower than that observed in the carbonaceous chondrite Acfer 094 [5, 6]. According to the O-isotopic composition ($\delta^{17}\text{O} = 70 \pm 140$ ‰, $\delta^{18}\text{O} = 640 \pm 80$ ‰), the grain belongs to the rare group 4 of oxide grains [7]. Both high metallicity AGB stars and type II supernovae are considered potential sources for the grains of this group [7, 8].

Preliminary inspection of the C and N data reveals the presence of a presolar C-rich grain, probably SiC, with $\delta^{13}\text{C} = 450 \pm 80$ ‰ and $\delta^{15}\text{N} = -310 \pm 130$ ‰ and size of ~ 250 nm, representing an abundance of 12 ppm of the matrix material. In addition we observed areas with ^{15}N -enrichments ($\delta^{15}\text{N}$ of up to 600 ‰), possibly representing molecular cloud material. A similar observation was made by [9] for chondritic organic matter.

Although the relatively low abundance of presolar silicates may be the result of aqueous alteration, the presence of different presolar minerals confirms the primitive nature of Tagish Lake.

Acknowledgements: We thank M. Zolensky for the Tagish Lake thin section, Elmar Gröner for technical support on the NanoSIMS, and J. Huth for SEM studies.

References: [1] Zinner E. 2004. In *Treatise on Geochemistry*, Elsevier, Oxford: pp. 17-39. [2] Brown P. G. et al. 2000. *Science* 290: 320-325. [3] Grady M. et al. 2002. *MAPS* 37: 713-735. [4] Mostefaoui S. et al. 2004. Abstract #1593. 35th Lunar and Planetary Science Conference. [5] Nguyen A. and Zinner E. 2004. *Science* 303: 1496-1499. [6] Mostefaoui S. and Hoppe P. 2004. *ApJ* 613: L149-L152. [7] Nittler L. R. et al. 1997. *ApJ* 483: 475-495. [8] Choi B.-G. et al. 1998. *Science* 282: 1284-1289. [9] Nittler L. R. et al. 2005. This volume.

CONCERNING THE IMPORTANCE OF RECOIL IN UNDERSTANDING PRESOLAR NANOGRAINS

E. Marosits¹, J. Maul² and U. Ott¹. ¹Max-Planck-Institut für Chemie, Becherweg 27, D-55128 Mainz, Germany (marosits@mpch-mainz.mpg.de). ²Institut für Physik, Johannes Gutenberg-Universität, D-55099 Mainz, Germany.

Introduction: Recoil effects may be of importance in the study of presolar grains in a variety of ways. It is essential, e.g., to understand recoil losses in spallation reactions in order to determine presolar cosmic ray exposure ages [1]. Recoil does also occur in radioactive decay, however. For β -decays it is usually a negligible effect, but the situation may be different for grains that are of nm-size such as the presolar nanodiamonds, where the expected evidence for the former presence of now extinct ^{26}Al and ^{44}Ti has not been found [2]. We have set out to experimentally determine whether loss due to recoil may be an explanation for this lack. This will eventually involve determining the actual retention of decay products such as ^{22}Ne from implanted ^{22}Na . Here we report on a pilot experiment in which Br in terrestrial nanodiamonds was converted into ^{82}Kr by irradiation with thermal neutrons.

Experimental: We used terrestrial detonation nanodiamonds supplied by A.P. Koscheev (cf. [3]) with a Br content determined as ~ 3 ppm by neutron activation analysis. The diamonds were washed with HNO_3 to remove surficial Br, suspended as a colloid in ammonia and then irradiated in the TRIGA reactor of the University of Mainz for 6 hours at a flux of $7 \times 10^{11} \text{ n cm}^{-2} \text{ sec}^{-1}$. After irradiation diamonds and liquid were separated, and the distribution of the ^{82}Br ($T_{1/2} = 35.34 \text{ h}$) between solid and liquid was determined by counting its γ -activity.

Results and Discussion: In several experiments we found the activity to be almost exclusively contained in the liquid phase, with the solid diamonds accounting for less than 20%. Loss at this stage is due to recoil during emission of prompt γ -rays. Assuming the grains to be spherical, we have compared the observed loss with a “predicted loss” calculated from the full spectrum of prompt γ -rays [5], the TRIM code for range-energy relation and the size distribution (mean $\sim 4.1 \text{ nm}$) of our explosion nanodiamonds (K2) as determined by MALDI-TOF-MS (similar to [6]). The “calculated” loss of $\sim 50\%$ is lower than what is observed, which may indicate that the TRIM Code underestimates ranges in nanometer-sized grains. This conclusion in no way is firm, however, and further experiments are required. It is clear, in any case, that the application of I-Xe dating [7] is problematic. It also appears possible that the reason for “missing” radionuclides in [2] is recoil loss. Losses appear to be not as severe, however, as required to achieve by this mechanism the “early separation” suggested as an explanation for the composition of Xe-H in presolar diamonds [8].

Acknowledgments. The authors thank the staff of Institut für Kernchemie and A.P. Koscheev for their cooperation.

References: [1] Ott U. and Begemann F. 2000. *Meteoritics & Planetary Science* 35:53-63. [2] Besmehn A. et al. 2000. Abstract #1544. 31th Lunar & Planetary Science Conference. [3] Koscheev A. P. et al. 2001. *Nature* 412:615-617. [4] Ziegler, J. F. 2003. *Nuclear Instruments and Methods in Physics Research B* 219-220, 1027-1036. [5] *Nuclear Data Sheets* 50 (1987):32-37. [6] Lyon, I. C. 2001. *Meteoritics & Planetary Science* 36:A119-A120. [7] Holland G. et al. 2003. *Meteoritics & Planetary Science* 38:A123. [8] Ott U. 1996. *Astrophysical Journal* 463:344-348.

TRAPPING OF XENON UPON EVAPORATION-CONDENSATION OF ORGANIC MATTER UNDER UV IRRADIATION: ISOTOPIC FRACTIONATION AND ELECTRON PARAMAGNETIC RESONANCE ANALYSIS.

Y. Marrocchi^{1,2}, F. Robert³, L. Binet⁴ and B. Marty¹. ¹CRPG-CNRS, Vandoeuvre-Lès-Nancy, France. ²Laboratory for Space Sciences, Washington University, Saint Louis, USA (ym@physics.wustl.edu). ³Laboratoire de Minéralogie, CNRS, MNHN, Paris, France. ⁴LCBOP, ENSCP/CNRS, Paris, France.

Introduction: Meteoritic noble gases are mainly hosted by two carbon-rich phases that are left after demineralization of bulk meteorite by HF and HCl: nanodiamonds and an enigmatic phase labeled as phase Q [1]. Phase Q is the carrier of P1 noble gases often referred to as 'planetary' and represents the majority of Ar, Kr and Xe trapped in primitive meteorites [1]. The mechanism leading to the trapping of P1 is poorly understood but may represent 2D trapping on surfaces. Here we report an experiment designed to study the trapping of Xe by sublimation-condensation process of anthracite. This experiment allowed us to probe the influence of irradiation on:

(i) the trapping of Xe onto organic matter, (ii) the EPR signal of organic matter synthesized by evaporation-condensation.

Experimental method: Anthracite was loaded in a crucible surrounded by a W filament [2]. UV light was located above the crucible. Air-like Xe was introduced in the system at a pressure of about 0.1 mbar and ionized with an energy of ≈ 0.1 MeV by high frequency discharge. The crucible was heated at 1200°C for 5 min and cooled down to room temperature immediately. Organic matter was condensed on the different glass parts of the apparatus with two kinds of samples recovered, corresponding to ionized xenon or neutral xenon.

Results: The amount of Xe trapped in ionized samples is about one order of magnitude higher than the one trapped in neutral samples. Neutral samples show the same xenon isotopic composition as the one of starting Xe. In contrast, ionized samples present an important isotopic fractionation of 1%/amu. The EPR spectra as a function of temperature allow the spin concentration to be estimated. Both samples present the same trend characterized by a decrease of spin concentration with increasing temperature. No significant difference was observed between neutral and ionized samples despite the drastic difference in condensation conditions.

Discussion: The isotopic fractionation observed could be induced by a charge exchange accompanied by an isotopic exchange: $m\text{Xe} + n\text{Xe}^+ \leftrightarrow m\text{Xe}^+ + n\text{Xe}$. Apparently, the organic matter during its condensation is able to realize a selection between neutral and ions Xe with a slight enhancement for trapping ions. The isotopic fractionation reproduces well the one observed for P1 noble gases relative to solar composition [1]. This result is consistent with previous works in which isotopic fractionation was observed only during experiments involving irradiation [3]. The decrease of spins concentration upon temperature determined for both samples is at odds with spins increasing upon temperature obtained for Orgueil and Murchison [4]. The present results suggest that condensation alone does not allow the diradicaloids of IOM to be produced. Interstellar chemistry seems to be the most promising process to reproduce the EPR characteristics. These results do not exclude a solar origin for P1 noble gases.

References: [1] Lewis R.S. *et al.* (1975) *Science* 190, 1251-1262. [2] Tissandier L. *et al.* (2002) *Meteoritics* 37, 1377-1390. [3] Hohenberg C.M. *et al.* (2002) *MPS* 37, 257-267. [4] Binet L. *et al.* (2004) *GCA* 68, 881-891.

A NEW METHOD FOR MEASURING THE EXTENT OF THERMAL METAMORPHISM IN ORDINARY CHONDRITES.

C. A. Marsh, D. S. Lauretta, and K. J. Domanik. Lunar and Planetary Lab, University of Arizona, Tucson, Arizona 85721, USA E-mail: celinda@lpl.arizona.edu

Introduction: Thermal metamorphism in ordinary chondrites (OCs) is quantitatively defined by homogeneity of olivine and low-Ca pyroxene [1]. In meteorite research homogeneity is measured using Percent Mean Deviation (PMD) and Coefficient of Variance (CoV) [2, 3]. Measuring the degree of heating primitive meteorites experienced is a critical step in understanding the mechanism(s) that heated planetesimals in the early solar system. Also, accurately measuring the fayalite and ferrosilite abundances in meteorites is necessary before robust links between asteroid and meteorite compositions can be established, especially if those links rely on near infrared spectra [4].

Technique: We have developed a calibrated x-ray mapping technique to quickly measure ferromagnesian silicate homogeneity within individual thin sections [5]. A routine in the Cameca task language was created that allows us to collect raw x-ray intensities of Fe, Mg, Ca and Si on 16,384 discrete 10 micron diameter footprints. We are continuing to test grid spacing between analyses in order to reduce selection bias. This technique does a better job of representing the homogeneity of the area mapped than the typical selection of a couple of points.

Data: As part of our study of progressive thermal metamorphism among the L-chondrites, we selected Allan Hills 77197 for examination. ALH 77197 is a 20.3 g meteorite that has been classified as an L3.7 with an A/B weathering stage. The olivine in ALH 77197 has an average composition Fa 28, a PMD of 5, and a CoV of 7. We found the low-Ca pyroxene in ALH 77197 to have an average Fs 17, a PMD of 19, and a CoV of 23. The ratio of Olivine to Orthopyroxene (Ol/Opx) is 6.2 for ALH 77197, indicating a low abundance of orthopyroxene. The highest Ol/Opx ratio measured by similar mapping techniques is 2.6 for an LL5 [6]. A BSE image taken at the same time that the elemental abundance mapping was conducted confirms the paucity of pyroxene in the mapped region. However, visual inspection of the thin section of ALH 77197 we are studying reveals the presence of a 2mm diameter radial pyroxene chondrule nearby.

Discussion: Ol/Opx ratios, along with average fayalite and ferrosilite content, are used as a proxy for oxidation state [7]. While these three values are linked, within a sample experiencing heat they will reach equilibration at different scales at different times. The data from ALH 77197 indicate that olivine has equilibrated and is highly oxidized for an L chondrite. Preliminary results show that both the Ol/Opx ratio and low-Ca pyroxene are not in equilibrium. Understanding the kinetics of equilibration in the olivine orthopyroxene system in ALH 77197 and similar meteorites will improve our ability to constrain the intensity and duration of thermal metamorphism.

References: [1] Van Schmus, W.R. and Wood, J.A. (1967) *GCA* 31: 747-765. [2] Dodd, R.T., *et al.* (1967) *GCA* 31: 921-951. [3] Scott, E.R.D. (1984) *Smithson. Contrib. Earth Sci* 26: 73-94. [4] McCoy, T.J. and Burbine, T.H. (2005) In *Workshop on Oxygen in Asteroids and Meteorites*, p. 22. [5] Marsh, C.A., *et al.* (2004) *Meteoritics & Planetary Science*, 39: A62. [6] Gastineau-Lyons, H.K., *et al.* (2002) *Meteoritics & Planetary Science* 37: 75-89. [7] Mccsween, H.Y., Labotka, T.C. (1993) *GCA* 57: 1105-1114.

EXTINCT ^{244}Pu ON THE MOON. K. Marti, C. Black, K.J. Mathew, Univ. of California, San Diego; Dept. Chemistry (0317), 9500 Gilman Drive, La Jolla, CA 92093-0317. kmarti@ucsd.edu

Information from extinct elements is particularly pertinent for filling the time gap between 3.9 and 4.5 Ga of lunar history, during which time the early bombardment of the inner solar system had taken place. Although there are several reports documenting the existence of extinct ^{244}Pu on the Moon, its potential use for collisional chronologies, as well as the initial abundance ratios have not been well assessed. This is in part due to the fact that some fission xenon components were found to be surface-correlated and not produced in-situ, and also because the presence of large cosmic-ray-produced components in most studied lunar rocks make the identification of fission Xe components difficult. We have identified rocks from Apollo 16(64455), 17(76010), and 14(14321) with well-resolved fission Xe components, suitably high REE abundances, and relatively small neutron capture and spallation components. We have determined their CRE ages by the ^{81}Kr - ^{83}Kr method which yields values of 2.0, 15 and 25 Ma, respectively. In disentangling multiple components of spallation, fission and trapped Xe components we use approaches of the type that were successful for martian meteorites and for ancient terrestrial zircons [1]. The results for nakhlite source region show that fission gas was assimilated starting with the early differentiation of Mars to the time of magma eruption 1.3 Ga ago [2,3]. The approaches are based on isotopic correlations which attempt to resolve fission data into components due to ^{244}Pu and ^{238}U , respectively, and which permit an estimation of the ^{244}Pu abundance at the time of system closure. When coupled to radiogenic age data, this permits an estimate of initial lunar ^{244}Pu abundance.

References: [1] Turner, G. et al. 2004. *Science* 306, 89-91. [2] Mathew, K.J. and Marti, K. 2001. *Journal Geophysical Research*, 106, 1401-1422. [3] Marti, K. and Mathew, K.J. 2004. *Antarctic Meteorite Research*, 17, 117-131.

AMINO ACIDS COMPOSITION AND OXYGEN ISOTOPES IN THE SHISR 033 CR CHONDRITE

Z. Martins¹, R. C. Greenwood², I. A. Franchi², O. Botta³, P. Ehrenfreund¹, B. A. Hofmann⁴ ¹Astrobiology Lab, Leiden Institute of Chemistry, P.O. Box 9502, 2300 RA Leiden, The Netherlands E-mail: z.martins@chem.leidenuniv.nl ²PSSRI, Open University, Milton Keynes, MK7 6AA, UK ³International Space Science Institute, Hallerstrasse 6, CH-3012 Bern, Switzerland. ⁴Natural History Museum, Bernastrasse 15, CH-3005 Bern, Switzerland

Shisr 033 is the first CR chondrite recovered in Oman. It consists of 65 fragments with a total mass of 1098 g collected from an area of a few square meters. The meteorite shows medium weathering of metal (W2) with omnipresent Fe-hydroxide staining. Compared with ¹⁴C-dated ordinary chondrites from Oman the degree of weathering is consistent with a terrestrial age of 5-15 kyr. Many fine-grained phyllosilicate-rich inclusions containing pyrrhotite and framboidal magnetite are apparent. The second largest fragment (249.9 g) was selected and 23 g of interior material were obtained by splitting away surface material. After gentle crushing, 4.86 g of fines enriched in phyllosilicate-rich material was selected for amino acids analysis. Selected individual phyllosilicate-rich clasts were analyzed by pyrolysis. From the coarse material individual chondrules were selected for O isotope analysis.

The acid hydrolyzed hot water extracts of the fines enriched in phyllosilicate-rich material were analyzed for amino acids using hot water extraction, followed by acid hydrolysis, desalting and pre-column derivatization [1]. Amino acids separation was achieved by high-performance liquid chromatography (HPLC) and by gas chromatography-mass spectrometry (GC-MS). Amino acid abundances were determined by comparison of the chromatographic signals with those of known standards. Shisr 033 contains extraterrestrial amino acids, including α -aminoisobutyric acid (AIB); however, comparisons to the CM2 Murchison, the CI Orgueil, and the CR Renazzo show a distinct amino acid distribution for this meteorite. The D/L ratio determined for alanine indicates the presence of terrestrial contamination.

Oxygen isotopic analyses were performed on a bulk sample (B), a bulk sample leached with ethanolaminthioglycollate to remove iron hydroxides (B2), a sample of composite chondrules (H) and a hand-picked dark clast (D). Samples B, B2 and H fall onto the CR trend as defined by Clayton and Mayeda (1999) [2]. The uncleaned bulk sample is significantly heavier than the cleaned one, most likely indicating an influence by terrestrial Fe-hydroxides (calculated $\delta^{18}\text{O}$ around +8‰ in equilibrium with Oman desert rainwater). The dark clast (D) falls onto the CV-CO trend. Stepped combustion of a dark clast revealed a low organic carbon and high carbonate contents indicative of terrestrial contamination.

References: [1] O. Botta and Bada J. L. 2002. *Surveys in Geophysics* 23: 411-467. [2] R. N. Clayton and T. K. Mayeda. 1999. *Geochimica et Cosmochimica Acta* 63: 2089-2104.

NOBLE GASES IN THE NEWLY FOUND CHASSIGNITE NWA 2737.

B. Marty¹, A. Grimberg², V.S. Heber² & R. Wieler², ¹CRPG-CNRS Nancy France. E-mail: bmarty@crpg.cnrs-nancy.fr. ²Isotope Geology, ETH Zurich, Switzerland.

Introduction: Although more than 30 Martian meteorites have been recognized so far, the Chassigny meteorite which fell in 1815 has remained unique in its clan. Recently, a 611 g meteorite located in the Moroccan desert was found to present striking similarities with Chassigny. Indeed it is a dunite (89.6 % olivine) displaying Mn/Fe in olivines and pyroxenes comparable to those of other SNC and a $\Delta^{17}\text{O}$ value of +0.305 [1]. However the meteorite differs from Chassigny by its higher Mg# (78.7 vs. 69) and its absence of plagioclase, thus demonstrating a different petrogenesis and possibly a different sampling area on Mars. The meteorite has informally been known as Diderot [1]; its approved name is NWA 2737.

Results: Here we present the results of a noble gas study of NWA 2737, aimed to document (i) the cosmic ray exposure ages, (ii) the occurrence of a solar noble gas component in the Martian mantle, only documented otherwise by the isotopic composition of Xenon in Chassigny [2,3], and (iii) the presence of Xe isotopes produced by the fission of ²⁴⁴Pu [3], a unique tracer to characterize both the heterogeneity of the Martian mantle as well as the degassing history of Mars [4]. In detail, solar-like Xe was released from Chassigny at relatively low temperature (<500°C), which is still unexplained given the refractory nature of its minerals, as well as during melting, in this case mixed up with almost chondritic proportion of plutogenic xenon [3]. In a pilot study we have measured light noble gases in order to determine CRE ages. ³He_c, ²¹Ne_c and ³⁸Ar_c are 9%, 13% and 41% higher in NWA 2737 relative to Chassigny, respectively. The similarity, within uncertainties, of the ³He_c and ²¹Ne_c contents between the two meteorites support identical exposure ages and therefore a common impact event. The higher ³⁸Ar_c content of NWA 2737 compared to Chassigny may be due to the small sample size used here which may not warrant homogeneity in Ca, a major ³⁸Ar producing element. A K-Ar age of 1.29 Ga (assuming no trapped ⁴⁰Ar) confirms the suspicion that NWA 2737 is indeed the second Chassignite. Further noble gas analysis is underway and data will be discussed at the conference.

[1] Beck P. et al. 2005. Abstract #1326. 36th Lunar & Planetary Science Conference. [2] Ott U. 1988. *Geochimica et Cosmochimica Acta* 52: 1937-1948. [3] Mathew K.J. and Marti K. 2001. *Journal of Geophysical Research* 106: 1401-1422. [4] Marty B. and Marti K. 2002. *Earth and Planetary Science Letters* 196: 251-263.

SPECTRA AND PETROGRAPHY OF EUCRITES AS A GUIDE TO ASTEROIDAL BASALTS. R. G. Mayne¹, J. M. Sunshine², T. J. McCoy³, and H. Y. McSween Jr. ¹Dept. of Earth and Planetary Sciences, Univ. of Tennessee, Knoxville, TN 37996-1410. (rmayne@utk.edu) ²SAIC, Chantilly, VA 20151 ³Dept. of Mineral Sciences, Smithsonian Institution, Washington DC, 20560-0119

Introduction: One of the significant challenges facing both the DAWN mission to 4Vesta and understanding lithologic differences among smaller basaltic asteroids (e.g., Vestoids) is interpreting spectral data in the context of the well-known chemical and textural groups of HEDs. Our group [1,2] is addressing this by conducting coordinated spectral, mineralogical and, textural studies of unbrecciated, Antarctic eucrites.

Methodology and Results: We selected MAC 02522, EET 87520, and ALH A81001 on the basis of differences in grain size, mineral compositions, modes and textures. Spectra of <45 μm powders were collected at RELAB and analyzed visually and with MGM [3]. EET 87520 is a slowly-cooled magnesian basaltic eucrite [4], whose spectrum is poorly fit by a single pyroxene, yet well-fit by two. The clear presence of both high- and low-Ca pyroxenes is consistent with its cooling history, while the positions of the absorptions are consistent with magnesian composition. The high-Ca pyroxene required to model the 2 μm region, necessitates the inclusion of an absorption near 1.2 μm . The addition of another band near 1.25 μm (attributable to plagioclase) does not significantly improve the fit. The spectrum of the medium-grained, heavily-shocked MAC 02522 is well fit with a single pyroxene in agreement with the lack of observed exsolution. Relative to EET 87520, the band centers shift to longer wavelengths, consistent with its iron-rich pyroxene composition [5]. The spectrum of vitric-textured ALH A81001 exhibits weaker bands. Modeling using a single calcic pyroxene is consistent with its composition. The reduced spectral contrast and the poor fit at ~0.4-0.8 μm likely results from the presence of fine-grained (few μm in size), dark ilmenite throughout the sample.

Implications and Caveats: This preliminary work suggests that spectral mapping of Vesta can identify units that differ in pyroxene composition. To a lesser extent, we may be able to distinguish slowly-cooled eucrites with exsolved pyroxenes from rapidly-cooled eucrites with calcic compositions with or without finely-dispersed oxides. This trend, if confirmed by extending this study, might provide a means of mapping partial melting or fractional crystallization across Vesta. We emphasize that the observed differences are largely relative. Incomplete calibrations for pyroxene compositions or mineral proportions (especially in plagioclase, high-Ca and low-Ca pyroxene mixtures) presently limit our ability to extract quantitative data. In particular, the relative influence of plagioclase and high-Ca pyroxene on spectral features is poorly understood. To relate to observable spectral features, future petrologic studies of HED's should focus on quantifying high- and low-Ca pyroxene ratios, as well as plagioclase to pyroxene ratios.

Acknowledgements: We acknowledge Takahiro Hiroi and Carlé Pieters for the collection of spectra at RELAB.

References: [1] Mayne R. G. et al. 2005. Abstract #1791. 36th Lunar and Planetary Science Conference. [2] Mayne R. G. et al. 2004. Meteoritics and Planetary Science 39:A65 [3] Sunshine J. M. 1990. JGR 95:6955-6966 [4] Antarctic Meteorite Newsletter. 1998. 11-2 [5] Adams J. B. 1974. JGR 79:4829-4836

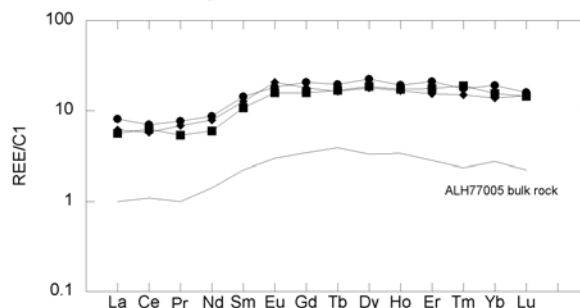
MELT REE CONTENTS OF IHERZOLITIC SHERGOTTITE ALH77005 AND NAKHLITE MIL03346: APPLICATION OF THE Eu-OXYBAROMETER. M. C. McCanta¹, M. J. Rutherford² and C. Calvin². ¹Lunar and Planetary Institute, Houston, Texas. E-mail: McCanta@lpi.usra.edu. ²Brown University, Providence, Rhode Island.

Introduction: To model the formation and evolution of a planet an understanding of the interior oxygen fugacity (f_{O_2}) of the planet is vital. For bodies other than Earth, measurements of this parameter are made in meteorites. Because of difficulties in measuring Martian meteorite f_{O_2} by conventional means a new oxybarometer was calibrated using the Eu content of pyroxenes and their coexisting melts [1]. Use of this oxybarometer relies on accurate knowledge of the REE content of the equilibrium melt composition. Melt is rarely present in these meteorites requiring bulk rock REE values to be substituted for melt compositions. For the basaltic shergottites, which appear not to have experienced significant crystal fractionation, this method appears sound. For the cumulate Martian meteorites, the lherzolitic shergottites and nakhlites, bulk rock melt compositions are more problematic. This study explores two cumulate meteorites, ALH77005 and MIL03346, which have had their melt inclusions and groundmass experimentally rehomogenized [2]. Unlike volatile elements, which may escape during remelting, the REE are fairly immobile and therefore provide potentially robust primary melt REE analyses. The melt REE contents measured in these samples allows for calculation of the crystallization f_{O_2} of these two meteorites.

Experimental and Analytical Methods: Small portions of ALH77005 and MIL03346, including melt inclusions, were rehomogenized as described in [2]. REE measurements were made on the Cameca-6F ion microprobe at Arizona State University.

Results: REE concentrations measured in ALH77005 rehomogenized melt inclusions are shown in the figure below. The pattern is consistent with bulk rock REE concentrations [3], but more enriched. The REE concentrations are similar to those measured in melt glass pockets in the Grove Mountain 99027 lherzolitic shergottite [4]. Values calculated from poikilitic low-Ca pyroxene core values indicate a crystallization f_{O_2} of IW+0.7. This f_{O_2} lies within the range of values measured in the basaltic shergottites (IW-0.6 to IW+1.9)[1]. Preliminary analyses suggest MIL03346 may have crystallized at a higher f_{O_2} value.

References: [1] McCanta *et al.* (2004) *GCA* 68, 1943-1952. [2] Calvin C. and Rutherford M.J. (2004) *34th LPSC*. [3] Ma *et al.* (1981) *Proc. Lunar Planet. Sci.* 12, 1349-1358. [4] Hsu W. *et al.* 2004 *Met. Planet. Sci.* 39, 701-709.



THE EARLY CRYSTALLIZATION HISTORY OF THE AUBRITE PARENT BODY. T.J. McCoy¹, A. Gale¹ and T.L. Dickinson². ¹Dept. of Mineral Sciences, National Museum of Natural History, Smithsonian Institution, Washington, DC 20560-0119 USA. E-mail: mccoy.tim@nmnh.si.edu. ² Space Studies Board, National Academies, 500 5th St. NW, Washington DC 20001.

Introduction. Aubrites are pyroxenites formed by basaltic partial melting and melt extraction, followed by complete melting of the residue and crystallization. The earliest stage of this final crystallization is poorly understood, although phases that crystallized prior to pyroxene (olivine, roedderite) are found. It is unclear how these phases were stabilized in a melt derived from olivine-poor enstatite chondrites. Further, the highly-brecciated nature of most aubrites makes deciphering the relationship between individual grains difficult. The discovery of an unbrecciated, olivine-bearing aubrite (LAP 03719) may shed light on this stage of aubrite history.

Results. LAP 03719 contains ~15 vol.% of slightly-rounded, unzoned forsterite crystals up to 2 mm in size enclosed in enstatite. The enstatite crystals include blebby diopside, reach up to 1 cm in length, and are intergrown at enstatite-enstatite boundaries. Polymineralic inclusions in olivine and enstatite up to a few hundred microns contain troilite, daubreelite, ferroan alabandite, kamacite and taenite.

Discussion. Three models are currently offered to explain the origin of olivine in aubrites:

(1) Olivine could form as a consequence of reduction of SiO₂ in the silicate melt to Si in the metallic phase at high-temperature [1]. Thus, one might expect metallic inclusions trapped in and formed before olivine to be Si-rich. However, metallic inclusions in olivine in LAP 03719 are Si-poor, although it is unclear if they sample this highest temperature melt.

(2) Olivine crystallization might be stabilized by crystallization of roedderite in a peralkaline aubrite melt [2]. The occurrence of roedderite and olivine in igneous contact [3] supported this model. However, olivine-bearing LAP 03719 lacks roedderite. Further, roedderite crystals in Pena Blanca Spring do not occur with olivine, exhibit evidence for resorption, and are rimmed by enstatite, diopside and plagioclase. A localized peralkaline melt evolved to metaluminous compositions, leading to roedderite resorption and plagioclase and djerfisherite crystallization.

(3) The inference of exsolved pigeonite in aubrites and the inability to crystallize pigeonite from an E6 melt could indicate aubrite formation from a precursor that differs from known enstatite chondrites [4]. Since LAP 03719 challenges two major theories to explain the origin of aubrites by melting of known enstatite chondrites, it is quite possible that a protolith unlike known enstatite chondrites is required. However, a re-examination of olivine-bearing unequilibrated enstatite chondrites [5] as a potential protolith is warranted.

References: [1] McCoy T.J. et al. (1999) *MAPS* **34**, 735-746 [2] Fogel R.A. (2001) *LPSC XXXII*, Abstract #2177 [3] Hsu W. (1998) *MAPS* **33**, 291-301. [4] Taylor G.J. et al. (1998) *LPSC XIX*, 1185. [5] Weisberg M.K. et al. (2005) *LPSC XXXVI*, #1420.

MINOR ELEMENT ZONING IN NAKHLITES: WHAT'S GOING ON? G. McKay¹ and T. Mikouchi². ¹Astromaterials Research Office, NASA Johnson Space Center. Gordon.mckay@jsc.nasa.gov. ²University of Tokyo.

Introduction: Nakhrites are olivine-bearing clinopyroxene cumulates. Based on petrographic characteristics, they may be divided into groups that cooled at different rates and may have been formed at different depths in a single flow [e.g., 1]. The order of cooling rate is Lafayette < Governador Valadares ~ Nakhla < Yamato000593 < NWA817 ~ MIL03346. Nakhrite cumulus pyroxene grains consist of large cores that are nearly homogeneous in major element composition surrounded by thin rims that are zoned to Fe-rich compositions. Detailed study of these pyroxenes is important because they retain a record of the crystallization history of the nakhrite magma. Moreover, because the composition of the nakhrite parent melt cannot be directly determined, the major and minor element composition of the cumulate pyroxene cores can be used to estimate the composition of that melt. This abstract reports some complications in the minor element zoning patterns of nakhrites.

Results: Elemental mapping of nakhrite pyroxenes reveals previously unrecognized zoning complexities. In the slowly cooled nakhrites, Al concentrations have a bimodal distribution, with one mode at ~ 0.4 wt % Al₂O₃ and another at ~0.9%. The spatial distribution of Al-rich and Al-poor regions is somewhat patchy, but is clearly subject to crystallographic control. Ti zoning is strongly correlated with Al. In contrast, Al is nearly homogeneous in the pyroxene cores of the rapidly cooled nakhrites NWA and MIL.

Cr is also zoned in both rapidly and slowly cooled nakhrites, but its spatial distribution bears no relationship to the Al and Ti zoning. Cr tends to be lowest in the center of the cores, and highest in the outer portions, reaching concentrations of ~ 0.35 wt % Cr₂O₃ in MIL, for example, before dropping off in the extreme outer portions of the cores.

Discussion: What is the origin of the Al and Ti zoning? One possibility is primary magmatic sector zoning. We have seen similar zoning in synthetic pyroxenes from our nakhrite experiments. But if it is primary in origin, why isn't it also found in the rapidly cooled nakhrites? The implications in this case are that there are major differences not only in late cooling, but also during the growth of the cumulus crystals. [2] reported that MIL contains a large amount of ferric Fe. Perhaps ferric Fe influences charge balancing and Al substitution during pyroxene growth and is present in lesser amounts in the slowly cooled nakhrites. Another possibility is that the zoning is secondary in origin, produced during subsolidus cooling. This could explain the difference between rapidly and slowly cooled nakhrites. However, in this case, why would the zoning be crystallographically controlled? Moreover, this could not be the origin of the zoning in our experiments. Another mystery is why is Cr zoning totally independent from that of Al and Ti? At the present time, we have more questions than answers. Additional detailed study, combined with additional crystal growth experiments are required to understand these complex zoning patterns.

References: [1] Mikouchi *et al.* (2005) LPSC 36. [2] Dyar *et al.* (2005) LPSC 36, #1261.

ODYSSEY GRS AND SNC METEORITE EVIDENCE FOR MULTIPLE LIL-ENRICHED RESERVOIRS ON MARS

S. M. McLennan¹, B. C. Hahn¹, W. V. Boynton² and G. J. Taylor³.
¹Dept. of Geosciences, SUNY, Stony Brook, NY, 11794-2100, USA. E-mail: Scott.McLennan@sunysb.edu. ²Lunar and Planetary Lab., Univ. of Arizona, Tucson, AZ, 85721. ³Hawaii Inst. Geophysics and Planetology, Honolulu, HI, 96822.

Introduction: Based on SNC meteorite geochemistry, the bulk composition of Mars generally is thought to be enriched in moderately volatile elements (*e.g.* K, Rb) compared to Earth [1]. This enrichment leads to K/U and K/Th ratios thought to be about double those of terrestrial primitive mantle. McLennan [2] questioned the degree of volatile enrichment in the martian primitive mantle on the basis of more recently obtained SNC analyses and suggested that the martian crust may constitute a LIL-enriched, low K/Th and low K/U reservoir that is not well-sampled by SNC meteorites. However, recent results from Mars Odyssey gamma ray spectrometer [3] confirm high K/Th ratios for the martian surface. This paper discusses some of the implications of this result.

SNC Meteorites: Many SNC meteorites possess high K/U (>15,000) and K/Th (>4000) ratios [1] compared to most terrestrial basalts (K/U~10,000; K/Th~2700). However, the young basaltic shergottites, comprising the majority of SNCs, are variably depleted in LREE and thus likely were derived in part from highly depleted mantle [2,4]. K/U and K/Th ratios decrease systematically with both K abundances and La/Sm ratios in basaltic shergottites [2]. These relationships suggest that a LIL-enriched, low K/Th reservoir forms a second component being sampled by basaltic shergottites.

Odyssey GRS K-Th Relationships: Odyssey GRS data suggest that the average martian surface is characterized by high K₂O abundances (0.40%) and high K/Th ratios (5500). Regional variations from these averages among geologically distinct terrains are only on the order of ±25% for K and ±10% for K/Th [3]. If representative of the entire crust, these values would imply that the martian crustal reservoir constitutes roughly half of the planet's complement of K and Th [3,5]. The high K/Th ratio would preclude this crustal reservoir from being the LIL-enriched component sampled by basaltic shergottites.

Discussion: There are several ways to explain the combined GRS and SNC meteorite K-Th systematics. GRS data may not be representative of the entire crust due either to crustal differentiation and/or stratification or to surficial processes fractionating K from Th. Although these possibilities cannot be excluded, the simplest interpretation is that GRS data are indeed representative of at least a significant fraction of the upper martian crust. If so, an additional LIL-enriched reservoir must exist, in either the mantle or crust, that is characterized by relatively low K/Th ratios (≤3000) and presumably low K/U ratios (≤12000). The size of the reservoir cannot be constrained but would be approximately proportional to the size of the depleted mantle reservoir sampled by basaltic shergottites.

References: [1] Wänke, H. and Dreibus, G. 1988. *Philosophical Transactions of the Royal Society of London* A325: 545-557. [2] McLennan, S. M. 2003. *Meteoritics and Planetary Science* 38: 895-904. [3] Taylor, G. J., Boynton, W. and 21 others. 2005. *Journal of Geophysical Research* (submitted). [4] Jones, J. H. 2003. *Meteoritics and Planetary Science* 38: 1807-1814. [5] McLennan, S. M. 2001. *Geophysical Research Letters* 28: 4019-4022.

FISSION XENON IN TRINITITES. A. P. Meshik, O. V. Pravdivtseva, and C. M. Hohenberg. McDonnell Center for the Space Sciences and Physics Department of Washington University, 1 Brookings Drive, Saint Louis, MO 63130 (am@physics.wustl.edu)

Trinitite is not a natural mineral; it is a result of flash heating of the sand at ground zero at nuclear test sites. Trinitite was first found 60 years ago at Trinity in Jornada del Muerto, southeast of Socorro, NM. Earlier analyses of similar material revealed Xe isotopic anomalies, with ^{132}Xe and ^{131}Xe being significantly enriched compared to ^{134}Xe and ^{136}Xe [1]. Here we report new measurements of even larger Xe anomalies in two trinitites (IF-2 and IG-2) and present a quantitative model for the mechanism by which they were formed.

Table. $^{136-131}\text{Xe}$ anomalies in trinitites. Isotopes $^{130-124}\text{Xe}$ have normal atmospheric composition. Xe from n-induced fission is shown for reference.

Sample (distance from the epicenter)	Temp. of max. Xe release	$^{132}\text{Xe} = 1$		
		^{136}Xe	^{134}Xe	^{131}Xe
IF-2 (<10 m)	1390°C	0.017 ±0.005	0.128 ±0.002	16.1 ±0.2
IG-2 (~100 m)	1320°C	0.006 ±0.004	0.145 ±0.003	3.17 ±0.06
[1] (unknown)		0.012 ±0.008	0.188 ±0.002	1.12 ±0.02
^{235}U fission		1.47	1.82	0.671

Observed anomalous Xe was evidently produced by two processes: (1) neutron induced fission of ^{235}U in the sand and (2) rapid temperature-activated diffusion of immediate fission products (mainly beta-active Sb). When the molten sand cools down and solidifies (forming trinitite), effectively terminating Sb diffusion, the accumulation of Xe isotopes in the trinitite is determined by the free decay of Sb. The observed Xe composition corresponds to 17 minutes cooling time for IF-2, and 5 minutes cooling time for IG-2. The release profiles of anomalous Xe indicate that IF-2 was previously heated to ~1390°C and IG-2 to ~1320°C. The virtual absence of ^{136}Xe is indicative of a neutron burst, since ^{135}I has a relatively long half-life.

Therefore the anomalous Xe in trinitites extends our knowledge about isotopic fractionation of fission xenon from temperature variations [2] and can be used for estimation of cooling path of U-bearing materials exposed to nuclear test neutrons. We will discuss a possible implication of these results for isotopic structure of Xe-HL in meteoritic nanodiamonds.

Trinitite samples were provided by Mineralogical Research Company. Supported by NASA grant NAG5-12776

References: [1] Pravdivtseva O. V. et al. 1986. *Proceedings of IX All-Union Symposium on Isotopes in Geochemistry*, 289, Moscow. [2] Meshik A. P. et al. 2003. *Meteoritics & Planetary Science* 38, A119.

PRE- AND POST-SUPERNOVA NUCLEOSYNTHESIS OF COSMOCHEMICALLY SIGNIFICANT ISOTOPES IN MASSIVE STARS.

B. S. Meyer. Department of Physics and Astronomy, Clemson University, Clemson, SC 29634-0978, USA. E-mail: mbradle@clemson.edu.

Introduction: Stars maintain their pressure support against gravitational collapse by burning nuclear fuel. This burning occurs in a complicated sequence of core- and shell-burning stages that may or may not be convective. By the time a massive star (i.e., one with mass 10 times greater than our Sun) has burned the initial hydrogen and helium in its core into the iron-group isotopes, it has a complicated structure that may be viewed as a series of concentric shells of differing isotopic composition. At this point, nuclear reactions will absorb rather than release energy, so the star becomes unstable to rapid gravitational collapse.

Collapse of the iron core of the massive star occurs on a timescale of seconds and halts only when the material reaches nuclear matter density. Material from stellar layers outside the core continues to reign down on the core supersonically. This launches a shock wave that works its way out through the outer layers of the star, heats and compresses them, and ejects them into the interstellar medium. Shock passage and interaction of neutrinos emitted from the newly-born neutron star with envelope material can change the isotopic composition of the matter in significant ways. For a review, see [1].

Nucleosynthesis: While the general picture of nucleosynthesis in massive stars is by now well understood, some details of the production of cosmochemically interesting isotopes such as ^{26}Al , ^{60}Fe , and ^{182}Hf remain to be explored fully. To study these issues, we have evolved a model of an initially 25 solar mass star with initial solar composition, modeled its explosion, and followed the attendant nucleosynthesis [2]. We find that the yield of ^{26}Al is sensitive in interesting ways to the treatment of the isomeric state in the isotope. In our calculation, we use internal transition rates as derived from [3]. We also find that pre-supernova synthesis of ^{60}Fe and ^{182}Hf can be greater than we previously expected. In our model, this strong production occurs in a non-convective helium-burning region just inside the convective helium-burning shell. In non-convective regions, neutron-capture flow can branch across unstable ^{59}Fe and ^{181}Hf . By contrast, in the convective helium-burning shell, newly-produced ^{59}Fe and ^{181}Hf rapidly move into regions of lower neutron density and decay before capturing another neutron, leading to much lower pre-supernova production of ^{60}Fe and ^{182}Hf in these zones. The convective history of the star thus plays an important role in the production of these isotopes.

After shock passage, the ^{60}Fe and ^{182}Hf abundances are modified but remain high. Some ^{60}Fe and ^{182}Hf is destroyed in the non-convective presupernova regions, but new ^{60}Fe and ^{182}Hf is produced in the outer regions.

Links at our web site

<http://nucleo.ces.clemson.edu>

provide further details of our model.

References: [1] Woosley S. E. et al. 2002. *Rev. Mod. Phys.* 74:1015–1071. [2] Meyer B. S. 2005. *PASP*. In press. [3] Gupta S. S. and Meyer B. S. 2001. *Phys. Rev. C*. 64:025805.

COMPARATIVE MINERALOGY OF CHASSIGNY AND NWA2737: IMPLICATIONS FOR THE FORMATION OF CHASSIGNITE IGNEOUS BODY(S). T. Mikouchi. Department of Earth and Planetary Science, University of Tokyo, Hongo, Bunkyo-ku, Tokyo 113-0033, JAPAN. E-mail: mikouchi@eps.s.u-tokyo.ac.jp.

The recent discovery of the second chassignite NWA2737 (NWA) can offer us a good opportunity to better understand the petrogenesis and formation history of this interesting Martian meteorite group [1-3]. Both Chassigny (CHA) and NWA are cumulate dunites having nearly identical modal abundances (90 % olivine with small amounts of pyroxene, chromite, and feldspathic glass). The olivine grain sizes are also similar (1-2 mm in size) and some grains show 120° triple junctions. The NWA olivine is more Mg-rich (Fe_{79-80}) than that of CHA (Fe_{69-70}). The Ca contents of olivine also slightly differ between them (CHA: 0.25-0.05 wt% and NWA: 0.2-0.05 wt%). Olivine grains in both samples show Ca decrease at their rims in spite of their homogeneous Fe-Mg compositions. The widths of zoned rims are about 150 μm for each sample and gave similar cooling rates (30 °C/year for 1150-650 °C). Chromite and melt inclusions commonly occur in olivines of both meteorites and their size and abundances are generally similar. It is striking that melt inclusions in both meteorites contain kaersutite amphiboles ($TiO_2 \sim 7$ wt%), although NWA kaersutite has a higher Mg/Fe ratio as host olivines. Pyroxenes in NWA melt inclusions are also more Mg-rich than that of CHA. Therefore, overall bulk composition of the NWA melt inclusion would be more Mg-rich than that of CHA. The interstitial areas to cumulus olivine are mainly composed of pyroxene, chromite, and feldspathic glass in both meteorites and their textures are similar. However, the chromite size is clearly larger in NWA (100-200 μm) than that of CHA (usually <100 μm). The chromite composition is also different and the NWA chromite has a higher Mg/Fe ratio. Pyroxenes display generally similar mineralogy between two meteorites although NWA pyroxene is more Mg-rich as other phases. Feldspathic glass in both meteorites has a nearly identical composition in major elements. Thus, general mineralogy and petrology are remarkably similar between these two chassignites. The largest difference between them is more magnesian composition of constituting phases in NWA as well as its higher shock metamorphism. It is likely that they originated from the same igneous unit on Mars as nakhlites. If not, the formation of cumulate dunite with variable Fe-Mg compositions may be common on Mars. Because the obtained burial depths are identical for these two chassignites, the latter may be preferred.

References: [1] Floran R. J. et al. 1978. *Geochimica et Cosmochimica Acta* 42:1213-1229. [2] Mikouchi T. et al. 2005. Abstract #1944. 36th Lunar & Planetary Science Conference. [3] Beck P. et al. 2005. Abstract #1326. 36th Lunar & Planetary Science Conference.

SEM-EBSD ANALYSIS ON SYMPLECTIC INCLUSION IN THE QUE93148 OLIVINE. T. Mikouchi¹ and K. Righter².

¹Department of Earth and Planetary Science, University of Tokyo, Hongo, Tokyo 113-0033, JAPAN. E-mail: mikouchi@eps.s.u-tokyo.ac.jp. ²Mail Code KT, NASA Johnson Space Center, Houston, TX 77058, USA.

QUE93148 is a small (1.1 g) achondritic meteorite mainly composed of olivine (Fo₈₆) with lesser amounts of orthopyroxene (En₈₅Wo₂), kamacite, troilite and chromite. It was originally classified as a lodranite, but its detailed chemistry and mineralogy rather suggest a relationship to pallasites [1,2]. One of the unique features of olivine petrology of QUE93148 is the presence of several different types of inclusions [1]. Among them, thin, lamellar inclusions (type 1 inclusion in [1], ca. 100 x 5 μm in size) are rare and it is not clear if there is one or two phases within the lamellae, because of their small size. In order to identify the phase(s) in the lamellae, and determine associated crystallographic information, we report FEG-SEM (field emission gun scanning electron microscopy) observation and EBSD (electron backscatter diffraction) analysis of these inclusions in olivine from this unique meteorite (PTS: QUE93148,11).

The FEG-SEM observation showed that these inclusions were clearly composed of two different phases exhibiting a sub-micron-scale symplectic texture similar to type 2 and especially type 3 inclusions [1]. EDS analysis by FEG-SEM showed that one phase was enriched in Cr and the other was enriched in Ca compared to the host olivine, suggesting that they are chromite and diopside, respectively [3]. We analyzed each phase by EBSD equipped with FEG-SEM in order to confirm the constituting phases. The analyzed areas were about 0.2-0.3 μm in scale. We could successfully obtain EBSD patterns for each phase. One of them could be indexed by chromite structure and the other was by diopside. Each phase in the same inclusion showed the same pattern (or orientation) in spite of the complex symplectic texture. This result is consistent with the symplectite crystallography demonstrated by TEM for the Nakhla olivine [4].

Thus, the type 1 inclusion in QUE93148 olivine is confirmed as symplectic mixture of chromite and diopside by SEM-EBSD. The symplectite texture of this inclusion is much smaller (sub-micron-scale) than the type 2 inclusion (micron-scale) which is composed of chromite and orthopyroxene with minor amounts of augite. As is pointed out by [1], the metal-sulfide grain in the type 2 inclusion acted as nucleation site and allowed it to grow larger than the others. Although this meteorite is important because of its unique chemistry and mineralogy suggesting a new type of pallasite [1,2], its small mass could limit analytical methods. In this study, the EBSD analysis was employed for a regular PTS and we could obtain crystallographic information without working on TEM. Hence, EBSD is a powerful analytical method when a small amount of samples is available (e.g., sample return mission).

References: [1] Goodrich C. A. and Righter K. 2000. *Meteoritics & Planetary Science* 35:521-536. [2] Floss C. 2002. *Meteoritics & Planetary Science* 37:1129-1139. [3] Righter K. and Delaney J. S. 1997. *Meteoritics & Planetary Science* 32:A108. [4] Mikouchi T. et al. 2000. *Meteoritics & Planetary Science* 35:937-942.

INSIDE OF THE FLYNN CREEK IMPACT AND PROCESSES OF CENTRAL UPLIFT FORMATION: THE VIEW FROM HAWKINS IMPACT CAVE

K. A. Milam¹, B. Deane¹, P. L. King², P. C. Lee³, and M. Hawkins⁴, ¹Dept. Earth & Planetary Sciences, Univ. of Tennessee, 306 EPSB, Knoxville, TN 37996-1410, kmilam@utk.edu, ²Univ. of Western Ontario, Dept of Earth Sci., London, ON, N6A 5B7, Canada, ³SETI Inst., NASA Ames Res. Center, Moffett Field, CA 94035-100, ⁴DeKalb Co. H.S., Smithville, TN 37166.

Introduction: Hawkins Impact Cave (HIC) is one of few caves in the world developed in a central uplift of a complex crater. Discovered in 1989 by landowner Michael Hawkins (name-sake) and mapped (277 m long) in 2003 [1], HIC lies in the core of the central uplift of the 3.8 km Flynn Creek impact crater (36°17'N, 85°40'W) in the Highland Rim physiographic province of north-central Tennessee, U.S. The 360 Ma impact occurred in flat-lying limestones, dolostones, and shale of the Lower Ordovician Knox Dolomite and Middle Ordovician Stones River Group [2]. Following impact, rocks were uplifted ~450 m above normal positions forming a central uplift [2-3]. Uplifted exposures consist primarily of westward dipping Stones River strata and lesser eastward-dipping rocks separated by a "chaotic breccia zone" [2].

Central Uplift Formation: Exposures in HIC provide a unique perspective into the processes of central uplift formation and their relative age relationships. Structural fabrics, similar to those observed in surface exposures of other central uplifts [4], are present in HIC. Bedding is dissected by extensive networks of listric microfractures (mfrs) and microfaults (mfs), indicating brittle failure of target rock during impact. Reverse and normal displacements (typically < 1 cm) along mfs represent localized compression and extension of target rock, likely during the contact/compression and modification stages of impact. Several sets of mfrs are cut by multiple generations of mfs. Monoclinic, anti-formal, and much more complex folds also occur with mfrs and mfs in large (up to several hundred m³) wedge-shaped megablocks of target rock.

Megablocks contain bedded to thinly-bedded carbonates with strike and dip orientations that vary from one block to the next. They are bound by narrow (< 1cm) major faults containing little or no breccia or cataclasis; dissimilar to fault breccias observed along major faults in other central uplifts. Major fault dissection of mfrs and mfs indicate subsequent movement after mfr/mf formation. Relative displacements are difficult to discern due to the paucity of slip indicators; however, drag folds are present along some major faults. Megablock rotation and transport likely occurred during uplift and subsequent collapse.

Development of HIC: Impact-related structures served as major controls on limestone dissolution and passage development in HIC. Water penetrated the cave from the southwest, preferentially dissolving limestone along major faults and at angles controlled by strike and dip directions of bedding inside of megablocks. As the water table continued to drop with base level, collapse along bedding planes and mfrs enlarged HIC passages. Passage morphology varies between megablocks and is affected by changes in structural fabric of the central uplift.

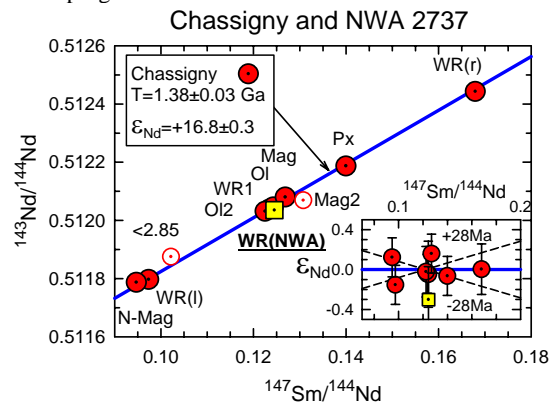
References: [1] Oeser et al. 2003, *TN Cave Survey*, Hawkins Impact Cave Map. [2] Roddy 1968, *Shock Met. of Nat. Materials*, Mono Books, pp. 291-322. [3] Roddy, 1979, *Proc. Lunar Planet Sci. 10th*, pp. 2519-2534. [4] Milam & Deane 2005, *LPSC XXXVI*, Abs. # 2161.

Rb-Sr AND Sm-Nd ISOTOPIC SYSTEMATICS OF NWA 2737 CHASSIGNITE. K. Misawa^{1,2} C.-Y. Shih³, Y. Reese⁴, L.E. Nyquist⁵ and J-A. Barrat⁶. ¹NRC Research Fellow, NASA Johnson Space Center, Houston, TX 77058, ²National Institute of Polar Research, Tokyo 173-8515, Japan. E-mail: misawa@nipr.ac.jp. ³Mail Code JE-23, ESCG/Jacobs Sverdrup, Houston, TX 77058, ⁴Mail Code JE-23, ESCG/Muniz Engineering, Houston, TX 77058, ⁵Mail Code KR, NASA Johnson Space Center, Houston, TX 77058, ⁶U.B.O.-I.U.E.M., place Nicolas Copernic, F-29280 Plouzané Cedex, France.

Introduction: NWA 2737 is the second Martian dunite composed of cumulate olivine (~90%), chromite (4%), pyroxene (5%) and interstitial sanidine (1%) [1,2]. To determine the crystallization age of NWA 2737 and to correlate the isotopic data with those of Chassigny, we have undertaken Rb-Sr and Sm-Nd isotopic studies of NWA 2737.

Analytical Procedures: A sample of NWA 2737, weighing ~2.3 g, was first washed with ethanol in an ultrasonic bath for 1 hour to remove brownish surface deposits, and then processed by gently crushing to grain size <149 μm . About 40% of the crushed material was taken as whole-rock samples (WR, WR1 and reserve). The WR1 sample was washed with 0.5N HCl in an ultrasonic bath for 10 minutes to leach out terrestrial contamination. Residue and leachate (WR1(r) and WR1(l)) plus an unleached sample (WR) were analyzed for Rb-Sr and Sm-Nd following the procedures of [3].

Results and Discussion: The Rb-Sr system of whole-rock samples was highly disturbed. The data for WR1(l), WR and WR1(r) plot to the left of the Chassigny isochron [4]. An elevation of $^{87}\text{Sr}/^{86}\text{Sr}$ ratios up to 0.7083 indicates an open system behavior of the Rb-Sr system due to the hot desert weathering. Abundances of Sm and Nd of the unleached sample (WR) are ~30% higher than those of Chassigny, which is consistent with the previous trace element data [1]. The Sm-Nd data for the unleached WR sample of NWA 2737 plots on the Chassigny isochron (Figure), suggesting that the chassignites may have almost identical crystallization age of ~1.38Ga. Additional analyses are in progress.



References: [1] Beck P. 2005. Abstract #1326. 36th Lunar & Planetary Science Conference. [2] Mikouchi T. et al. 2005. Abstract #1944. 36th Lunar & Planetary Science Conference. [3] Shih C.-Y. et al. 1999. *Meteoritics & Planetary Science* 34: 647-655. [4] Misawa K. et al. 2005. Abstract #1698. 36th Lunar & Planetary Science Conference.

ORIGIN OF MAIN-GROUP PALLASITES.

David W. Mittlefehldt, NASA/Johnson Space Center, Houston, TX, USA. david.w.mittlefehldt@nasa.gov.

Main-group pallasites (PMG) are mixtures of iron-nickel metal and magnesian olivine thought to have been formed by mixing at the core-mantle boundary of an asteroid [1]. Six have anomalous metal compositions (PMG-am); four have atypically ferroan olivines (PMG-as) [2]. In one model [2], the PMG metal is consistent with an origin as a late fractionate of the IIIAB iron core. Those with anomalous metal include refractory metal trapped in the dunite as a partial melt residue, or brought in with molten metal as solid grains of early crystallized metal nucleated on the core roof. The ferroan olivines were oxidized late by gases expelled from the crystallizing core. This model is based on PMG textures, metal compositions and olivine Fe/Mg. I have determined major, minor and some trace elements by EMPA and INAA in PMG olivines and use these data to further constrain their origin.

PMG olivines have experienced subsolidus redox reaction with the metal, which would alter their Fe/Mg [3]. Manganese is homologous with divalent Fe, and can be used to distinguish between magmatic and redox processes as causes for Fe/Mg variations. PMG olivines show a range in molar $1000 \cdot \text{Mn/Mg}$ of 2.3-4.2 indicating igneous fractionation in olivines with similar Fe/Mg. The Mg-Mn-Fe distributions could be explained by a fractional crystallization-reduction model. PMG with the lowest Mn/Mg are close to the initial olivine compositions. Fractional crystallization drove Mn/Mg and Fe/Mg to higher values. Subsolidus redox reaction with the metal decreased Fe/Mg to roughly uniform values, but preserved the fractionated Mn/Mg.

There is a crude positive association between Mn/Mg and Sc content; those with lower Mn/Mg have lower Sc and vice-versa. This is consistent with an igneous fractionation origin. The range in Sc contents (0.71-2.23 $\mu\text{g/g}$) could have resulted from ~33% fractional crystallization of an ultramafic magma. This is inconsistent with formation at the core-mantle boundary of a single asteroid [4]. An alternative is that the olivines are melt-residues; if the parent asteroid was initially heterogeneous, dunite residues at the base of the mantle could have different Sc contents and Mn/Mg, partly because of initial differences, and partly because of different degrees of melting. This model is ad hoc, although ureilites and acapulcoite-lodranite clan meteorites do suggest heterogeneous achondrite parent asteroids existed [1].

The sole PMG-as studied here - Springwater - is not easily fit in any scenario. Its olivine has a Mn/Mg as high as the highest PMG; there is no need to call on late oxidation to explain its high Fe/Mg [2]. However, it also has the lowest Sc content (0.53 $\mu\text{g/g}$) and is inconsistent with a fractional crystallization relationship with PMG. The combination of low Sc with high Mn/Mg violates the loose association between these observed for PMG, requiring greater initial heterogeneity to fit into the partial-melt residue model. Finally, if PMG have roughly uniform Fe/Mg because of redox exchange, why did PMG-as escape this?

If all main-group pallasites formed on a single parent asteroid, then the olivines are most likely melt-residues, and the parent asteroid was initially heterogeneous.

References: [1] Mittlefehldt et al. (1998) *Reviews in Mineralogy* 36, chp. 4. [2] Wasson & Choi (2003) *GCA* 67, 3079. [3] Righter et al. (1990) *GCA* 54, 1803. [4] Mittlefehldt (1999) *LPS XXX*, #1828.

A NEW IRON-NICKEL PHOSPHIDE FROM THE NORTHWEST AFRICA 1054 METEORITE. V. Moggi-Cecchi¹, L. Bindi², and G. Pratesi^{2,3}, ¹Museo di Scienze Planetarie, Provincia di Prato, Via Galcianese, 20/h, I-59100 Prato, Italy, e-mail: v.moggi@pratoricerche.it, ²Museo di Storia Naturale, Università degli Studi di Firenze, I-50121 Firenze, Italy, ³Dipartimento di Scienze della Terra, Università di Firenze, Via La Pira, 4, I-50121, Florence, Italy, e-mail: gpratesi@unifi.it

Introduction: NWA 1054 is a primitive achondrite (acapulcoite) with a main mass weighing 86 g. The thin section displays a granular texture with olivine and low-Ca pyroxene as major phases and high Ca-pyroxene and plagioclase as minor; major non-silicate phases are metal and troilite. Accessory phases include merrillite, a Mg-rich chromite and two iron-nickel phosphides. Terrestrial weathering grade is low (W1) as well as shock stage (S1). The Museo di Scienze Planetarie of Prato (MSP) owns the type specimen (MSP2366) [1].

Description: Six natural phosphides are known: schreibersite, $(\text{Fe,Ni})_3\text{P}$, nickelposphide $(\text{Ni,Fe})_3\text{P}$ [2], barringerite $(\text{Fe,Ni})_2\text{P}$ [3], allabogdanite $(\text{Fe,Ni})_2\text{P}$ [4], florenskyite FeTiP [5] and perryite, $(\text{Ni,Fe})_8(\text{Si,P})_3$ [6]. In the course of a study on some acapulcoites a new rather common iron-nickel phosphide was discovered in the NWA 1052 and 1054 acapulcoites [7]. The chemical composition of the new phase, determined by EMPA, is $(\text{Ni}_{2.30}\text{Fe}_{1.64}\text{Co}_{0.01})_{\Sigma=3.95}\text{P}_{1.05}$, pointing to a 4:1 metal/phosphorous ratio. It occurs as anhedral grains up to 100 μm either associated with kamacite (Fig. 1A) or with nickelposphide (Fig. 1B). Micro-indentation measurements provided a value (447 kg/mm^2) lower than nickelposphide. In reflected light, the new phase is cream-yellowish, non pleochroic, isotropic, and shows no bireflectance, without internal reflections. Reflectance values are 60.56, 50.44, 52.51 and 55.94 % at 471.1, 548.3, 586.6, and 652.3 nm, respectively. A single-crystal X-ray diffraction study, carried out on a small crystal fragment, indicates a cubic lattice with $a = 6.025 \pm 0.001$ and points to a space group $P2_13$ with $Z = 4$. Both the coordination-number (12) and the density (7.882 g/cc) are the highest ever reported for phosphorus and iron-nickel phosphides, respectively.

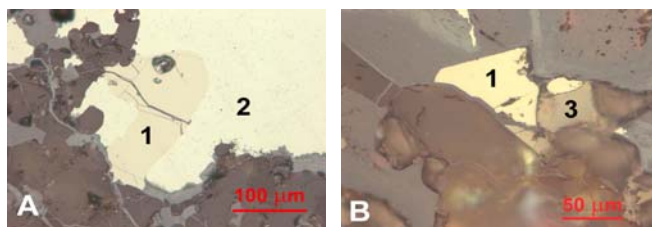


FIG. 1 Reflected light photographs displaying (A) the new phosphide (1) associated with kamacite (2) and (B) with nickelposphide (3).

Conclusions: The structure and the physical properties suggest that the new iron nickel phosphide could play an important role for Earth's core mineralogy. Due to the presence of this phase NWA 1054 acapulcoite seems to be a really peculiar acapulcoite if compared with literature data [8-9].

References: [1] Moggi Cecchi V. & Pratesi G. (2005) *MAPS*, **40**, in press [2] Skála R. & Drábek M. (2003) *Min. Mag.* **67**, 783 [3] Buseck P.R. (1969) *Science* **165**,169 [4] Britvin S.N. et al., (2002) *Am. Min.* **87**, 1245 [5] Ivanov A.V. et al., (2000) *Am. Min.* **85**, 1082 [6] Okada A. et al. (1988) *MAPS* **23**, 59 [7] Moggi-Cecchi V., Pratesi G., Mancini L., (2005) *LPSC. XXXVI*, abs. #1808 [8] Patzer A., Hill D.H., Boynton W.V. (2004) *MAPS* **39**, 61 [9] Scott E.R.D. & Pinault, L.J. (1999) *LPSC. XXX*, abs. #1507.

MID-INFRARED SPECTROSCOPY OF MATRIX MATERIAL FROM CHONDRITES: FIRST HEATING EXPERIMENTS. A. Morlok^{1,4}, M. Koehler^{2,4} and M. M. Grady^{3,4} ¹The Natural History Museum, Cromwell Road, London, SW7 5BD, UK. E-mail: A.Morlok@nhm.ac.uk. ²Institut fuer Planetologie, Wilhelm-Klemm-Str.10, 48149 Muenster, Germany ³PSSRI, Open University, Walton Hall, Milton Keynes, MK7 6AA, UK ⁴IARC

Introduction: Infrared spectroscopy is a way to compare laboratory data of planetary materials with those of astronomical observations. In our ongoing project [1] we systematically measure infrared spectra of minerals and components of meteorites, mainly for the comparison with spectra from dust material like circumstellar disks around young stars or comets. Here, we present first preliminary results of heating stage experiments with matrix materials separated from a variety of chondrites (Ornans CO3, Felix CO3, Allende CV3, Vigarano CV3, Ningqiang CK3, NWA978 CR, Kakangari K, Al Rais CR2, Cold Bokkeveld CM2 and Orgueil CI). While there are several infrared studies of bulk materials and matrices of meteorites [e.g. 2, 3], we provide additional information about the spectra of the materials at different temperatures. This gives insight into the change of such materials during heating processes e.g. in evolving, young solar systems.

Techniques: Matrix material was separated using a fine tungsten needle from polished blocks of meteorite sample under a binocular. It was tried to avoid larger mineral grains and other components. In the following, the materials have been ground to a sub-micron powder in a compression cell and placed on a KBr-disk in a LINKAM FTIR600 heating stage. This stage was mounted on a Perkin Elmer AutoImage FT-IR microscope. Spectra were taken in 100°C steps from room temperature to ~550 degree in transmission mode. The spectral range was from 2.5 to 16micron, limited by the ZnSe windows of the heating stage.

Results: The resulting preliminary spectra of the hydrated CI1 and CM2 meteorites are characterized by a single, big 'bulge'-like feature at ~9.9 micron, which is probably result of the dominating phyllosilicates.

The spectra of Ornans, Felix, Allende, Vigarano, Ningqiang and NWA978 are similar to olivine spectra at room temperature. Kakangari has characteristic spectra, with strong bands at 9.32, 9.89, 10.61 and 10.55 microns, probably a mixture of forsterite and enstatite features.

In the olivine dominated spectra the strong feature at ~11.3 micron hardly shifts with increasing temperature, while the smaller feature at ~10micron shifts towards higher wavelengths. Also the relative intensity changes, with increasing temperature the 11.3micron feature shrinks, while the feature at 10 micron grows relatively. The strong phyllosilicate features in the hydrated CI1 and CM2 chondrites shift from 9.9, 9.89 and 9.88 micron (for Cold Bokkeveld, Al Rais and Orgueil) to 10.32, 10.28 and 10.23 microns.

Acknowledgements: This work is supported by PPARC (A.Morlok) and EU/DFG (M.Koehler)

References: [1] Morlok A. et al. 2005. *Submitted to Planetary and Space Science*. [2] Sandford S. A. 1984. *Icarus* 60, 115-126. [3] Osawa T. et al. 2005. *Meteoritics & Planetary Science*, 40, 71-86

REVISED DATING OF ALAMO AND SOME OTHER LATE DEVONIAN IMPACTS IN RELATION TO RESULTING MASS EXTINCTION. J.R. Morrow¹ and C.A. Sandberg². ¹Dept. of Earth Sciences, Univ. of Northern Colorado, Greeley, CO 80639. E-mail: jared.morrow@unco.edu. ²U.S. Geological Survey, Box 25046, MS 939, Federal Center, Denver, CO 80225.

Introduction: The stepwise Late Frasnian (mid-Late Devonian) mass extinction is one of the five largest Phanerozoic extinction episodes. High-resolution data presented by numerous workers indicate that stepwise, progressive biodiversity loss is a fundamental characteristic of Phanerozoic mass extinctions. Late Devonian data, which must now be re-examined in light of new radiometric and conodont biochronologic dating, suggest that multiple sub-critical impacts coincided with significant biodiversity losses, culminating in an end-Frasnian mass extinction.

Late Devonian Impacts: The early Late Devonian Alamo impact is dated by conodont biochronology as early Frasnian *punctata* Zone. Previously this was converted to a date of ~367 Ma. However, recent radiometric dating by Kaufmann and colleagues [1,2] of the Late Devonian, which closely parallels dating by Tucker et al. [3], has necessitated redating the Alamo impact as ~382 Ma. The Alamo impact targeted a marine, off-platform (~300-m-deep) site in south-central Nevada [4]. Although the crater has been tectonically dissected and dislocated and later buried, the evidence for impact is well documented, e.g., [4,5,6,7]. Conodont dating of the Flynn Creek impact structure, Tennessee, by Schieber and Over [8] suggests the next older *transitans* Zone, ~1 m.y. older than the Alamo impact, although their recorded conodont species are permissive of a *punctata* Zone age. However, a critical conodont collection [9], now apparently lost, from a currently inaccessible outcrop within the structure may suggest an age younger than the *transitans* Zone. The Amönau possible impact event [10,11], Germany, is dated by conodonts as *falsiovalis* Zone, which is the next older, early Frasnian, pre-*transitans* zone. Calibration of the *falsiovalis* Zone age for the Amönau event against the revised Late Devonian time scale [1,2] indicates a numeric age of ~383.5 Ma. The Siljan impact, Sweden, is dated numerically as ~376.8 Ma +/- 1.7 m.y. [12]. This dating is either coincident with, or just before, the Late Frasnian mass extinction, at ~376.1 Ma +/- 1.6 m.y. [1].

Conclusion: These new numeric dates confirm that a series of Frasnian impacts, interpreted as comet showers [11], accompanied and probably promoted progressive, low-latitude biodiversity loss, culminating with ecosystem collapse that produced the end-Frasnian mass extinction.

References: [1] Kaufmann B. et al. 2004. *Journal of Geology* 112:495–501. [2] Trapp E. et al. 2004. *Geology* 32(10):857–860. [3] Tucker R. D. et al. 1998. *Earth and Planetary Science Letters* 158:175–186. [4] Morrow J. R. et al. 2005. *Geological Society of America Special Paper* 384:259–280. [5] Warme J. E. and Sandberg C. A. 1995. *Courier Forschungsinstitut Senckenberg* 188:31–57. [6] Leroux H. et al. 1995. *Geology* 23:1003–1006. [7] Warme J. E. and Kuehner H.-C. 1998. *Intl Geology Review* 40:189–216. [8] Schieber J. and Over J. D. 2004. *Geological Society of America Abstracts with Programs* 36(5):160. [9] Huddle J. W. 1963. *U.S. Geological Survey Professional Paper* 475C:C55–C57. [10] Ormö J. 1994. *Berg & Dal Bladet* 3:9–10. [11] Sandberg C. A. et al. 2002. *Geological Society of America Special Paper* 356:473–487. [12] Reimold W. U. et al. 2004. Abstract #1480. 35th Lunar & Planetary Science Conference.

EU ISOTOPIC VARIATIONS IN ALLENDE CAI.

F. Moynier¹, A. Bouvier¹, J. Blichert-Toft¹, P. Telouk¹, D. Gasperini² and F. Albarède¹. ¹ENS Lyon 46 allée d'Italie, 69007 Lyon, France fmoynier@ens-lyon.fr, ²Universita di Pisa, 56126 Pisa, Italy

Introduction: In this work, we determined the isotope composition of Eu, which has two isotopes ¹⁵¹Eu and ¹⁵³Eu, on a small number of samples of terrestrial material and meteorites. We demonstrate that natural variability in terrestrial and meteorites is well within analytical uncertainties but that a prominent anomaly is observed in Allende refractory inclusions.

Experimental methods: Samples were dissolved in a HF-HNO₃ mixture. Eu is purified by the combination of cation exchange resin and reverse-phase chromatography on HDEHP-coated fluoropolymer beads. The samples were analyzed on the VG Plasma 54 MC-ICP-MS of ENS Lyon. Sample external reproducibility on each ratio is 50 ppm and blank is 50 ng.

Results: On average, the ¹⁵³Eu/¹⁵¹Eu ratios of the terrestrial samples are constant and deviate from the standard by about -1 ε, which strongly suggests that the Eu standard was fractionated during manufacturing with respect to the Bulk Earth value. The values for the terrestrial samples, for the chondrules and the bulk meteorites are within error of the mean ε/amu value of -1. The ¹⁵³Eu/¹⁵¹Eu ratios of the Allende CAIs are -3.9, -5.5 and -5.9 ε/amu. The largest Eu isotopic anomaly observed in the CAI is therefore of -5.9 ε/amu. Murchison CAIs seems to be devoid of a significant anomaly.

Discussion: *Nucleosynthetic effects.* Very old stars with low metallicity ([Fe/H] ≤ 2.5), which are expected to have recorded a smaller number of nucleosynthetic events, have almost the same *r*-process abundance as the Sun (COHEN et al., 2003). In addition, it is unlikely that the CAI analyzed contain a substantial excess of *r*-process nuclides: although ¹⁵⁴Sm is more than 99% an *r*-process nuclide, its abundances in the same material show no identifiable excess.

Evaporation and condensation. A ¹⁵³Eu deficit is unlikely to be created by evaporation of a solid residue. It may in contrast develop if the CAIs are late condensates that only formed after a substantial fraction of the hot vapor had been drawn out from the system. For all elements, isotope fractionation reversal takes place after ~63 percent of the element was removed from the vapor. How so much isotopically heavy material remains unaccounted however remains unexplained and we feel that we can investigate alternative explanations.

Electromagnetic effects. Magnetic separation in the plasma surrounding the young Sun within ~0.1 AU is a plausible alternative interpretation of the reversed isotopic fractionation. Potassium is the main source of electrons and reaches full ionization at ~2000°C [2], such a temperature would certainly be attained at ~0.06 AU where [3] suggest that the CAI originated.

Although the actual ion velocity field is undoubtedly complex, the heavier isotopes of the ionized species move on trajectories of lesser curvature and should appear as being preferentially driven off the orbit of the parent neutral atoms and molecules. Electromagnetic separation could therefore turn isotopic variability into a probe of velocity field fluctuations in the solar nebula.

References: [1] W. Aoki et al., *Astrophysical Journal* 592, L67-L70, 2003. [2] T. Umebayashi, *Progress of Theoretical Physics* 69, 480-502, 1983. [3] F.H. Shu et al., *Science* 271, 1545-1552, 1996.

ZN ISOTOPIC MASS FRACTIONATION DURING HIGH TEMPERATURE SEGREGATION OF METAL FROM SILICATE. F.Moynier¹, T.Rushmer² and F.Albarède¹. ¹ENS Lyon 46 allée d'Italie, 69007 Lyon, France fmoynier@ens-lyon.fr, ²University of Vermont, Burlington VT 05405

Introduction: The moderate range (1‰) of Zn and Cu isotope variations of the magmatic iron meteorites IIIA and of the metal phases of the Brenham pallasite has been interpreted as the consequences of liquid metal-solid metal or silicate-liquid metal separation, i.e., the segregation of the core of the IIIA parent body [1]. The range of the Zn isotopic fractionation occurring during the silicate/metal separation still needs to be explored experimentally. This preliminary report describes isotopic fractionation of Zn between metal and silicate in partially molten chondritic material at high temperature and low pressure.

Analytical methods: Experiments were performed at 1 atm in a gas-mixing furnace at McGill University. For all the experiments the oxygen fugacity has been precisely fixed at the iron-wüstite buffer. A dozen of experiments have been prepared from 1000°C to 1300°C. Chunks of 300-400 mg of Kernouvé (H6 chondrite) were placed inside a platinum wire, and put into the furnace for 24 hours. The results of 48 hours and 24 hours experiments are in good agreement, which suggests equilibration. Zn isotope composition have been measured on the MC-ICP-MS P54 of the ENS Lyon [2].

Results and Discussion: The Zn isotopic fractionation between metal and silicate is reported as:

$$\Delta\delta^{66/64}\text{Zn} = (\delta^{66/64}\text{Zn})_{\text{silicate}} - (\delta^{66/64}\text{Zn})_{\text{metal}}$$

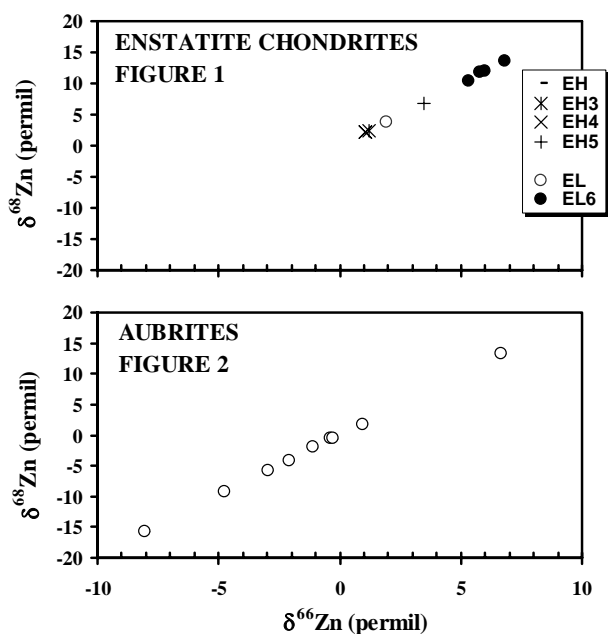
The external reproducibility on $\Delta\delta^{66/64}\text{Zn}$ measurements is 100 ppm. The range of $\Delta\delta^{66/64}\text{Zn}$ is 0.5 ‰. All the experiments show positive $\Delta\delta^{66/64}\text{Zn}$, which reflect that the silicate minerals are isotopically heavier in Zn than the metal phase. The silicate phases of the two pallasites are also isotopically heavier in Zn than the metallic phases ($\Delta\delta^{66/64}\text{Zn}=0.66-1.25\%$). The $\delta^{66/64}\text{Zn}$ values of both metal and silicate phase increases with the temperature, which indicates that, during the high temperature experiments, the lightest isotopes of the Zn are preferentially lost to the vapor. There is a weak correlation between the $\Delta\delta^{66/64}\text{Zn}$ and the temperature. The small Zn isotope fractionation ($-0.04 < \Delta\delta^{66/64}\text{Zn} < 0.15$) in the 1000°C experiments compares with metal-silicate fractionation in the original Kernouvé sample ($\Delta\delta^{66/64}\text{Zn}=0$ ‰). This suggests that, at 1000°C, Zn isotopes are not significantly fractionated. In contrast, Zn isotopes are fractionated in higher temperature experiments ($0.1 < \Delta\delta^{66/64}\text{Zn} < 0.5$), with a maximum fractionation at 1150°C and 1200°C. Such a fractionation compares with what is observed in pallasites ($\Delta\delta^{66/64}\text{Zn} = 0.66-1.25\%$). Our experiments confirms that isotopic fractionation in pallasites may reflect high-temperature segregation of metal from silicate [2] but does not reproduce the large Zn isotopic fractionation observed in these meteorites.

Reference: [1] Luck et al. (submitted) *Geochim. Cosmochim. Acta* [2] C. Maréchal et al. (1999) *Chem. Geol.* 156,251-273

EXTREME FRACTIONATION OF ZINC ISOTOPES IN ENSTATITE CHONDRITES AND AUBRITES. E. Mullane^{1,2}, S.S. Russell¹, M. Gounelle^{1,3} ¹Dept. Mineralogy, Natural History Museum, London SW7, U.K. ²Dept. Geology, The Field Museum, Chicago IL 60605. ³CSNSM-Université Paris 11, Bât.104, 91405 Orsay, France.

Introduction: Aubrites and enstatite chondrites (EC) are highly reduced meteorites. Zinc is a volatile element with 50% condensation temperature of 726 K [1] and bulk zinc isotope composition was measured by MC-ICP-MS. Laboratory and analytical procedures have been outlined elsewhere [2]. Precision at 95% confidence interval is $\delta^{66}\text{Zn} \pm 0.04$ and $\delta^{68}\text{Zn} \pm 0.08$.

Results: EC $\delta^{66}\text{Zn}_{\text{IRMM}} = +1.07$ to $+6.83$ permil. EL6 chondrites are isotopically heaviest and EH3 and 4 are lightest (Figure 1). In contrast to the EC, aubrites show a greater range of compositions and are both isotopically heavy and light with respect to the standard ($\delta^{66}\text{Zn}_{\text{IRMM}} = -8.04$ to $+6.68$ permil) [3].



The scale for each diagram is identical.
Error bars are smaller than the symbols.

Discussion: Zinc isotopes in EC become increasingly heavy with increased petrologic type, with a separation of over 1 permil/amu between EH3-4 and EH5 and between EH5 and EL6. However, the difference between EH and EL6 may reflect their origin on separate parent bodies e.g. [4]. One reason for the extreme fractionation of zinc isotopes in aubrites may be accounted for by impact volatilization of zinc. All of the studied aubrites are brecciated (except for Shallowater). If aubrites derive directly from EC then the isotopically light composition of many aubrites with respect to the EC-like protolith must be explained. The merits of the above processes, or combination of these processes, are the subject of our ongoing study.

References: [1] Lodders, 2003, *Astrophys. J.* 591, 1220-1247. [2] Mullane et al., 2005, *EPSL*, in press. [3] Mullane et al., 2005, *LPSC 36*, No.1250 and 1251. [4] Sears et al., 1982, *GCA* 46, 597-608.

FRACTIONATION OF IRON ISOTOPES DURING MAGMATIC PROCESSING ON THE IIIAB PARENT BODY.

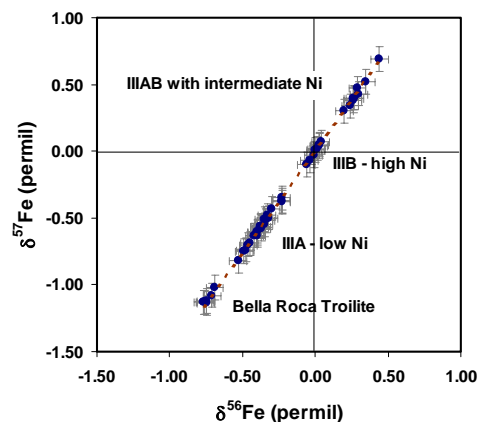
E. Mullane^{1,2}, S.S. Russell¹, M. Gounelle^{1,3} ¹Dept. Mineralogy, Natural History Museum, London SW7, U.K. ²Dept. Geology, The Field Museum, Chicago IL 60605. ³CSNSM-Université Paris 11, Bât.104, 91405 Orsay, France.

Introduction: Magmatic irons (including the IIIAB group) are believed to be the products of fractional crystallization of a molten asteroid core [1,2]. In an earlier study of Fe-isotopes in samples from differentiated asteroids we reported that Henbury was isotopically light [3] and that the metal component of pallasites was not uniform in isotopic composition [3,4]. The purpose of this study was to determine if IIIAB irons have a similar Fe-isotope composition to Henbury or if they have a range of isotope signatures, similar to those seen in pallasites, and to what extent fractionation may be controlled by segregation of immiscible sulphide melts during cooling and crystallization.

Samples & Methods: The Fe-isotope composition of 32 IIIAB irons (14% of the total IIIAB population) and a troilite nodule is reported. As IIIABs are medium octahedrites and contain relatively coarse kamacite lamellae, care was taken to sample material representative the bulk meteorite. MC-ICP-MS analytical techniques have been described previously [5]. Precision (95% confidence level) is $\delta^{56}\text{Fe} \pm 0.05$ and $\delta^{57}\text{Fe} \pm 0.07$ permil.

Results: The Bella Roca troilite nodule is isotopically light by 0.7 permil ($\delta^{56}\text{Fe}_{\text{IRMM}}$) with respect to its host IIIAB iron (Fig. 1). The isotopic range in IIIAB irons spans $\delta^{56}\text{Fe}_{\text{IRMM}}$ from -0.53 to $+0.44$ permil (Fig. 1).

Discussion: The Fe-isotope compositions are not systematic with respect to the fractional crystallization sequence. Early solids are Ni-poor and Ni content increases as crystallization advances. Early solids are isotopically light, late solids are relatively unfractionated and intermediate solids are isotopically heavy (Fig. 1). This behaviour is difficult to explain if the IIIAB group represent a single crystallizing magma. In addition, the iron isotope composition of the troilite nodule, which is a late crystallizing solid phase, is light (similar to the early solidified, low-Ni IIIABs). In conclusion, fractional crystallization is accompanied by iron isotope fractionation, but the reason for the non-systematic fractionation behaviour is unclear at present and will be the subject of continuing work.

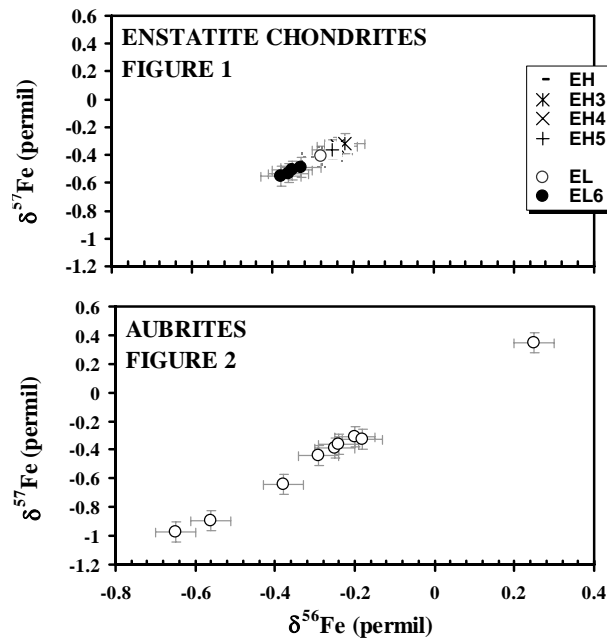


References: [1] Scott (1972) GCA 36, 1205-1236. [2] Malvin et al. (1986) GCA 50, 1221-1231. [3] Mullane et al., 2002, MAPS 37, A105. [4] Mullane et al., 2004, MAPS 39, A74. [5] Mullane et al., 2005, EPSL, in press.

IRON ISOTOPE COMPOSITIONS OF ENSTATITE CHONDRITES AND AUBRITES. E. Mullane^{1,2}, S.S. Russell¹, M. Gounelle^{1,3} ¹Dept. Mineralogy, Natural History Museum, London SW7, U.K. ²Dept. Geology, The Field Museum, Chicago IL 60605. ³CSNSM-Université Paris 11, Bât.104, 91405 Orsay, France.

Introduction: Aubrites and enstatite chondrites (EC) are very reduced meteorites. Iron is a moderately volatile element with 50% condensation temperature of 1334 K [1]. Iron isotopes were measured by MC-ICP-MS. Laboratory and analytical procedures have been outlined elsewhere [2]. Precision at 95% confidence interval is $\delta^{56}\text{Fe} \pm 0.05$ permil and $\delta^{57}\text{Fe} \pm 0.07$ permil.

Results: EC show a smaller range ($\delta^{56}\text{Fe}_{\text{IRMM}} = -0.38$ to -0.22 , $n = 9$, Fig. 1) than aubrites ($\delta^{56}\text{Fe}_{\text{IRMM}} = -0.65$ to $+0.25$ permil, $n = 9$, Fig. 2) [3,4]. This is a similar pattern to that seen for Zn-isotopes (see companion abstract). Excluding Bishopville the range in $\delta^{56}\text{Fe}_{\text{IRMM}}$ for aubrites is -0.65 to -0.18 permil.



Discussion: All EC are isotopically light compared to IRMM. EH chondrites are tightly clustered around $\delta^{56}\text{Fe}_{\text{IRMM}} = -0.23$ permil, EL6 chondrites range from $\delta^{56}\text{Fe}_{\text{IRMM}} = -0.33$ to -0.38 permil and Happy Canyon (EL) falls in the middle. Happy Canyon is an impact melt which has been heavily weathered [5], so terrestrial modification of its Fe-isotope signature cannot be ruled out [3]. EC Fe-isotope compositions could be either inherited from the nebula during accretion or be the product of post accretion processing such as metamorphism. Aubrites, may be the differentiated products of EC, or EC-like material [6]. Many aubrites have compositions similar to the EC but 3 are very distinct, possibly due to heterogeneous protolith material, melting or impact processing, or a mixture of these processes.

References: [1] Lodders, 2003, *Astro. J.* 591, 1220-1247. [2] Mullane et al., 2005, *EPSL*, in press. [3] Mullane et al., 2005, *LPSC* 36, No.1250. [4] Mullane et al., 2005, *LPSC* 36, No. 1251. [5] Keil, 1989, *Meteoritics* 24, 195-208. [6] Watters & Prinz (1979) *LPSC* 10, 1073-1093.

EXPERIMENTAL PETROLOGY OF OLIVINE-PHYRIC SHERGOTTITES: PRIMARY MANTLE MELTS? D. S. Musselwhite¹ and A. H. Treiman², Lunar and Planetary Institute, Houston, TX 77058, ¹musselwhite@lpi.usra.edu, ²treiman@lpi.usra.edu.

Introduction: The olivine-phyric basaltic shergottites (OPSs) have been recently recognized as a significant sub-group of the Martian meteorites. These rocks have many characteristics suggestive of a primitive nature such as high bulk and olivine core Mg#s [1]. [2,3] conducted crystallization experiments using the composition of Yamato 980459 (Y98), an OPS. Results of these experiments show that the olivine cores are in equilibrium with the bulk rock, indicating that the bulk-rock composition is the same as the parent melt. Multiple saturation of the melt with olivine and a low-calcium pyroxene occurs at 11.5 to 12 kbars and 1450 ± 10 °C indicating that the melt separated from the mantle at a depth of ~100 km. Experiments similar to [2,3] on the Gusev Crater basalt composition [4] found multiple saturation at a pressure of 11kbar -- nearly identical to the pressure for Y98, implying a similar lithospheric thickness under Gusev Crater. NWA 1068, another OPS may also represent a primary mantle-derived magma. Evidence for this comes from the composition of magmatic inclusions [5], olivine and pyroxene zoning [6], and the fact that the bulk Fe/Mg ratio is in equilibrium with the olivine cores [7]. Furthermore, calculations using the MELTS program of [8] predict multiple saturation at a similar pressure to Y98 and Gusev compositions.

Experimental Methods: Crystallization experiments are being conducted using a piston cylinder apparatus on a synthetic NWA1068 composition (Table 1) from [6] (corrected for the effects of desert weathering) at Martian mantle pressures and temperatures. The pressure assembly is comprised of a BaCO₃ cell, MgO internal parts, and C-type thermocouple. Oxygen fugacity is controlled using the method of [9] whereby starting material with a preset Fe₂O₃ content is loaded into a graphite capsule. Runs are analyzed using the Cameca SX-100 electron probe at NASA/JSC.

Table 1: composition of starting material (wt% oxide)

SiO ₂	46.17	MgO	16.67
TiO ₂	0.78	NiO	0.03
Al ₂ O ₃	5.81	CaO	7.44
Cr ₂ O ₃	0.64	Na ₂ O	1.15
FeO	20.69	K ₂ O	0.16
MnO	0.46	Total	100.00

Discussion: The object of these experiments is first to determine whether NWA 1068 is a primary mantle melt. Evidence for this will come from the composition of first-formed crystals and searching for multiple saturation on the liquidus. If it is a primary melt, then depth and temperature of source separation can be determined which will further constrain mantle thermal models. A positive outcome will have significant implications for geochemical models of SNC petrogenesis. In contrast to other OPSs, NWA1068 is undepleted. So if NWA 1068 is indeed a primary mantle melt, it would argue against crustal contamination as the source reservoir for the undepleted, oxidized end-member of the shergottites.

References [1] Meyer C. (2004) *Mars Meteorite Compendium 2004*. [2] Dalton, H.A. et al. (2005) *LPSC XXXVI* abs #2132 [3] Musselwhite, D.S. et al. (2005) *MAPS* (submitted) [4] Monders A.G. et al.(2005) *LPSC XXXVI* abs #2069 [5] Wadhwa M. and Crozaz G. (2002) *MAPS* **37**, A145. [6] Barrat et al. (2002) *GCA* **66**, 3505-3518 [7] Goodrich et al. (2003) *MAPS* **38**, 1773-1792 [8] Giorso, M. and Sack, R. (1995) *Cont Min Pet* **119**, 197-212. [9] Kress V. C. and Carmichael I. S. E. (1988) *Am Min* **73**, 1267-1274.